American Psychological Association

Journal of Experimental Psychology: General

ISSN: 0096-3445

2020, Vol. 149, No. 5, 949–966
http://dx.doi.org/10.1037/xge0000693

The Validated Circular Shape Space: Quantifying the Visual Similarity of Shape

Aedan Y. Li and Jackson C. Liang
University of Toronto

Andy C. H. Lee and Morgan D. Barense
University of Toronto and Rotman Research Institute at Baycrest Hospital, Toronto, Ontario, Canada

Subjective similarity holds a prominent place in many psychological theories, influencing diverse cognitive processes ranging from attention and categorization to memory and problem solving. Despite the known importance of subjective similarity, there are few resources available to experimenters interested in manipulating the visual similarity of shape, one common type of subjective similarity. Here, across seven validation iterations, we incrementally developed a stimulus space consisting of 360 shapes using a novel image-processing method in conjunction with collected similarity judgments. The result is the Validated Circular Shape space, the first Validated Circular Shape space comparable to the commonly used "color wheel", whereby angular distance along a 2D circle is a proxy for visual similarity. This extensively validated resource is freely available to experimenters wishing to precisely manipulate the visual similarity of shape.

Keywords: visual similarity, perceptually uniform, circular shape space, angular distance, mixture model

Supplemental materials: http://dx.doi.org/10.1037/xge0000693.supp

Certain items are more similar than others. For example, we can agree that a computer is more similar to a TV than to a dog. This similarity judgment can be made on the basis of perceptual attributes, such as the auditory (Aldrich, Hellier, & Edworthy, 2009), gustatory (Pfaffmann, Bartoshuk, & McBurney, 1971), olfactory (Guerrieri, Schubert, Sandoz, & Giurfa, 2005), tactile (Skedung et al., 2013), and visual properties of an item (Wardle, Kriegeskorte, Grootswagers, Khaligh-Razavi, & Carlson, 2016). Similarity judgments can also be made on the basis of abstract attributes, such as the functional properties of an item (Martin, Douglas, Newsome, Man, & Barense, 2018), the category of an item (Charest, Kievit, Schmitz, Deca, & Kriegeskorte, 2014; Jozwik, Kriegeskorte, & Mur, 2016), and the shared contexts that items are typically encountered in (Ezzyat & Davachi, 2014). Here, the tendency for observers to group items together on the basis of some characteristic or set of characteristics is known as *subjective similarity*. An extension to the construct of subjective similarity is *subjective variability*, whereby the similarity within sets of items can range from low to high. For example, the change in subjective similarity within one set (e.g., laptop, computer, TV, headset) can be less variable compared to another set (e.g., pen, dog, sofa, water bottle).

Subjective similarity has a rich history in psychological research (Attneave, 1950; Pothos, Busemeyer, & Trueblood, 2013; Tversky, 1977); it is known to broadly influence cognitive processes ranging from attention (Duncan & Humphreys, 1989) and categorization (Goldstone, 1994) to memory (Jiang, Lee, Asaad, & Remington, 2016; Sun, Fidalgo, et al., 2017; Yassa & Stark, 2011) and problem solving (Novick, 1988). Not only is subjective similarity frequently studied in behavioral experiments, subjective similarity is also a key property underlying how the brain supports cognition (Davis, Xue, Love, Preston, & Poldrack, 2014; Kriegeskorte, Mur, & Bandettini, 2008). Distributed patterns of neural activity map onto subjective similarity for both nonhuman and human primates, for stimuli ranging from simple lines to complex faces (Kaneshiro, Perreau Guimaraes, Kim, Norcia, & Suppes, 2015; Martin et al., 2018; Mur et al., 2013). Such findings have

This article was published Online First October 3, 2019.

Aedan Y. Li and Jackson C. Liang, Department of Psychology, University of Toronto; Andy C. H. Lee and Morgan D. Barense, Department of Psychology, University of Toronto, and Rotman Research Institute at Baycrest Hospital, Toronto, Ontario, Canada.

Earlier versions of this work were presented at the Lake Ontario Visionary Establishment in 2016, the Canadian Society for Brain, Behaviour and Cognitive Science in 2017; the Vision Sciences Society in 2017 and 2018; the Toronto Area Memory Group in 2018; and the Memory Disorders Research Society in 2018. This work formed part of the Master's thesis of Aedan Y. Li, a preprint is available at https://www.biorxiv.org/content/biorxiv/early/2019/01/31/535922, and the stimulus materials are shared on the Open Science Framework (https://osf.io/d9gyf/).

We thank Celia Fidalgo for her invaluable discussions and ideas regarding the development of the shape space, Tim Brady for helpful discussion and his suggestion to use multidimensional scaling for validation, as well as Keisuke Fukuda for commenting on an initial draft of this article. Aedan Y. Li is supported by an Alexander Graham Bell Canada Graduate Scholarship-Doctoral from the Natural Sciences and Engineering Research Council of Canada (NSERC). This work is supported by a Scholar Award from the James S. McDonnell Foundation, an Early Researcher Award from the Ontario Government, an NSERC Discovery grant and Accelerator supplement, and a Canada Research Chair to Morgan D. Barense. This work is also supported by an NSERC Discovery grant to Andy C. H. Lee.

Correspondence concerning this article should be addressed to Aedan Y. Li, Department of Psychology, University of Toronto, 100 George Street, Toronto, ON M5S 3G3, Canada. E-mail: aedanyue.li@utoronto.ca

spurred researchers to suggest that subjective similarity is an organizing principle of the cortex, whereby there is an isomorphism between neural and cognitive representations of the world (Davis et al., 2014; Kriegeskorte & Kievit, 2013).

Despite the known importance of subjective similarity, there is a paucity of available resources that allow experimenters the ability to precisely operationalize and manipulate the subjective similarity of stimuli. Traditional methods involve the use of experimenter-based intuition when designing stimuli or the use of image-processing methods to mathematically adjust the pixel-wise similarity between images (Busey, 1998). In particular, mathematical approaches have many advantages, including rapid stimulus development and the parametric manipulation of similarity. However, purely mathematical approaches also have drawbacks, as human observers do not always subjectively experience similarity the same way as a mathematical measure (Busey, 1998; Larkey & Markman, 2005), and thus subjective similarity may be inadequately captured. In some cases, this practice may be problematic if study conclusions depend on precise estimates of subjective similarity (Busey, 1998). In other cases, experimental conditions that differ drastically on the basis of subjective similarity or subjective variability may have later unintentional consequences on the interpretation of the data. For example, memories can be differentially influenced by subjective similarity: Memories can become blurred in conditions where stimuli are subjectively similar, whereas memories can become inaccessible in conditions where stimuli are subjectively dissimilar (Sun, Fidalgo, et al., 2017). Furthermore, conditions that differ on the basis of subjective variability cannot only differentially influence how items are remembered (Hanczakowski, Beaman, & Jones, 2017; Lin & Luck, 2009) but can also differentially alter how stimuli within each condition capture attention (Becker, Folk, & Remington, 2013). To control for undesirable stimulus-driven effects, experimenters typically counterbalance stimuli across conditions and participants, with the acknowledgment that this solution may reduce the power of finding desired outcomes.

Perceptually Uniform Spaces

In cases when counterbalancing is not possible or if a study design requires a precise measure of subjective similarity, experimenters typically collect similarity judgments in a domain such as visual similarity (Hout, Goldinger, & Ferguson, 2013; Martin et al., 2018; Kriegeskorte & Mur, 2012). In other cases, experimenters sample stimuli from an already established *perceptually uniform space*. Perceptually uniform spaces contain stimuli mapped to an *n*-dimensional space, whereby the spatial arrangement between stimuli approximates their relations of visual similarity. One popular example is CIELAB color space, a commonly used 3D perceptually uniform space (i.e., colors are defined on the basis of a luminance dimension, a green–red dimension, and a blue–yellow dimension) that mimics human trichromatic color vision (McDermott & Webster, 2012; Robertson, 1990). CIELAB space was developed and validated from foundational experiments conducted in the early 20th century, whereby just noticeable differences to color were derived from perceptual matching tasks (Brown & MacAdam, 1949; Guild, 1931; Wright, 1929). For this reason, CIELAB color space is a good approximation of visual similarity, though this stimulus space is not a perfect match to human color vision (Cheung, 2016). Indeed, increasingly sophisticated perceptually uniform color spaces have been developed to better account for visual similarity, though even these newer spaces are not perfectly analogous to color perception (Safdar, Cui, Kim, & Luo, 2017). It is important to emphasize that these perceptually uniform spaces control for only visual similarity and do not necessarily control for other types of subjective similarity. For example, cross-cultural differences in categorical color boundaries (Abbott, Griffiths, & Regier, 2016; Regier, Kay, & Khetarpal, 2007; Roberson, Davies, & Davidoff, 2000; Zaslavsky, Kemp, Regier, & Tishby, 2018), and other higher-order effects such as likability (Labrecque & Milne, 2012) can all influence color judgments beyond visual similarity (Taylor, Clifford, & Franklin, 2013). As with any tool, experimenters will need to weigh the positives and negatives to determine suitability for a given research question. Nevertheless, perceptually uniform spaces are highly useful, allowing for both the rapid stimulus selection afforded by mathematical approaches to similarity as well as a principled method to control for visual similarity, one common type of subjective similarity.

To simplify the stimulus set, experimenters often reduce the dimensionality of CIELAB color space to a 2D circular space (i.e., a "color wheel"; Figure 1A). By holding luminance constant, stimuli are then sampled from the circumference of a circle so that hue varies incrementally (Ma, Husain, & Bays, 2014). Importantly,

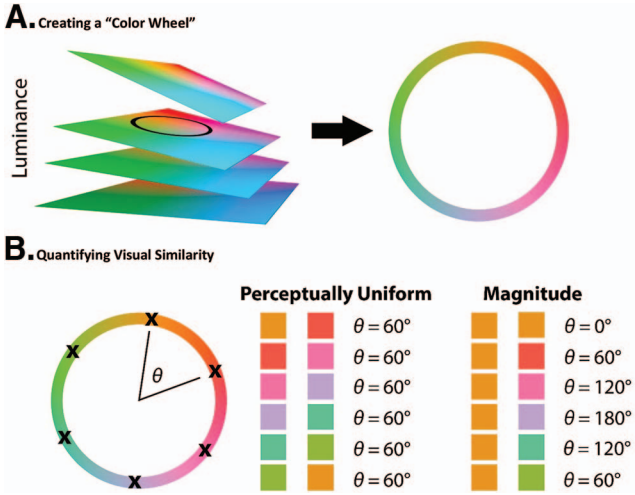

Figure 1. (A) Rendition of 3D CIELAB color space, whereby visual similarity can be approximated by the Euclidean distance between colors. After controlling for luminance on the *y*-axis of the figure above, a 2D circle can be defined so that hue varies incrementally. (B) There are two ways to consider visual similarity on a circular space. An ideal circular space is *perceptually uniform*, meaning that two items sampled from any distance are about as similar as any two other items sampled from the same distance. For example, pairs of stimuli in each row on the figure above are sampled every 60 degrees distance (θ). This property allows experimenters to equate the variation of similarity from one stimulus to the next. Second, on an ideal circular space, the magnitude of visual similarity can be approximated by angular distance. In the example above, pairs of colors (displayed in each row) sampled closer in angular distance tend to be more similar than pairs of colors sampled further away. This property allows experimenters to characterize the amount of visual similarity along a continuum. See the online article for the color version of this figure.

there are two ways to define similarity on circular color space (Figure 1B). First, the circular space can be said to be *perceptually uniform*, meaning that colors sampled from any distance apart are about as visually similar as any other colors sampled from that same degrees' distance. Using this property, subjective variability can be controlled by sampling stimuli from equidistant angular positions on circular space (i.e., using the perceptually uniform property; Figure 1B). Thus, the change in visual similarity from one stimulus to the next is equivalent across the set. Researchers in the vision sciences frequently apply this method to control the variation of visual similarity, such as when using color stimuli (Brouwer & Heeger, 2009, 2013; Zhang & Luck, 2008). The perceptually uniform property has also been useful in understanding how the brain supports color perception (Brouwer & Heeger, 2009, 2013). For example, the relational structure of circular color space was reconstructed from spatially distributed patterns of neural activity in area V4 and VO1 but not from earlier visual regions, even though earlier visual areas contained decodable information about color hue (Brouwer & Heeger, 2009). These results suggest that subjective color perception emerges from later areas of the visual processing stream, an example of how the perceptually uniform property of circular space can aid our understanding of the neural mechanisms involved in color perception.

Second, the magnitude of visual similarity can be approximated by angular distance on a circular space, meaning that colors sampled from closer distances tend to be more visually similar than colors sampled from further distances. Here, it is important to realize that there are two distinct properties on circular space. The perceptually uniform property captures information about the relations of visual similarity at the level of the set, in contrast, angular distance approximates how much similarity changes relative to a single item (i.e., using the magnitude property; Figure 1B). For example, relative to orange, colors positioned closer in angular distance (e.g., red) are more visually similar than colors positioned further in angular distance (e.g., blue). Depending on the research question, angular distance may be adequate as an approximation of the magnitude of visual similarity. However, for cases in which an experimenter wishes to precisely measure the magnitude of similarity between two items on circular space, a function can be built to convert from angular distance directly to visual similarity using collected similarity judgments (Schurgin, Wixted, & Brady, 2018; also see the *Step 6: Distance Function* section). In the memory literature, recent evidence suggests that participant responses from certain tasks (e.g., continuous retrieval task; Wilken & Ma, 2004) may be better described by analyzing responses using the magnitude of visual similarity rather than by angular distance on circular space (Schurgin et al., 2018). Though more research is needed to determine the measure that best describes memory in these tasks, we highlight that circular spaces have been useful in reconceptualizing and refining our understanding of the neural and behavioral underpinnings of memory (Cooper & Ritchey, 2019; Ma et al., 2014; Nilakantan, Bridge, VanHaerents, & Voss, 2018; Richter, Cooper, Bays, & Simons, 2016; Schurgin et al., 2018; Yonelinas, 2013). In this domain, circular spaces are often also used in conjunction with mixture models to estimate both the detail of memories as well as the probability of outlier responses that resemble random guesses (Ma et al., 2014; Richter et al., 2016; Zhang & Luck, 2008, 2009).

Building a Circular Shape Space

Circular spaces allow for both the control over subjective variability as well as the ability to capture visual similarity along a continuum. However, whereas experimenters have created and validated these stimulus spaces for color (Cheung, 2016; McDermott & Webster, 2012; Pointer, 1981; Robertson, 1977), a validated circular shape space does not yet exist, reflecting the lack of resources available to experimenters wishing to select shape stimuli well-controlled on the basis of visual similarity. Important previous attempts mathematically varied sets of sinusoidal curves (e.g., using Fourier descriptors, Zhang & Luck, 2008, or radial frequency patterns, Salmela, Mäkelä, & Saarinen, 2010), although these circular spaces were never validated in terms of visual similarity. Whereas mathematical measures such as radial frequency patterns have been shown to capture some of the variance in human similarity judgments for shape (Op de Beeck, Wagemans, & Vogels, 2001; Salmela, Henriksson, & Vanni, 2016), other researchers suggest that these measures may not reflect an organizing principle for shape representation more generally (Schmidtmann & Fruend, 2019). Indeed, the organization of shape in the visual system is an active and ongoing area of research (Bell, Hancock, Kingdom, & Peirce, 2010; Cacciamani, Scalf, & Peterson, 2015; Firestone & Scholl, 2014; Gallant, Braun, & Van Essen, 1993; Haushofer, Livingstone, & Kanwisher, 2008; Hung, Carlson, & Connor, 2012; Pasupathy, El-Shamayleh, & Popovkina, 2018; Peirce, 2015; Salmela et al., 2016; Sanguinetti, Allen, & Peterson, 2014).

In contrast to purely mathematical approaches, we used a novel iterative image-processing method to create a circular shape space explicitly validated using human-based similarity judgments. Here, we describe and characterize the Validated Circular Shape (VCS) space, the first perceptually uniform shape space whereby angular distance is a proxy for visual similarity. A set of 360 shapes was mapped onto 360 degrees of a 2D circle. This space was empirically validated to confirm that it was perceptually uniform (i.e., shapes sampled from any degrees' distance were about as visually similar as any other shapes sampled from the same degrees' distance). We then precisely quantified the relationship between angular distance and the magnitude of visual similarity, demonstrating that shapes sampled closer in angular distance were more visually similar than shapes sampled further away. VCS space is fully open source (available on the Open Science Framework: https://osf.io/d9gyf/), and this resource is provided to researchers interested in using shape stimuli extensively validated and quantified on the basis of visual similarity.

Method

We implemented a novel iterative validation procedure in which we (a) designed a set of initial shapes, dubbed "prototypes" (Figure 2A); (b) morphed between pairs of these prototypes to generate 360 unique shapes mapped onto each degree of a circle (Figure 2B); (c) collected similarity ratings (Figure 3A) and collated these ratings across participants (Figure 3B) within a group similarity matrix (Figure 3C); (d) used this group matrix to reconstruct shape space with multidimensional scaling (MDS; Figure 3D); and (e) identified problematic regions that were not circular (Figure 3E). Problematic shapes were iteratively corrected until a circular shape space could be created. For example, prototypes may have been

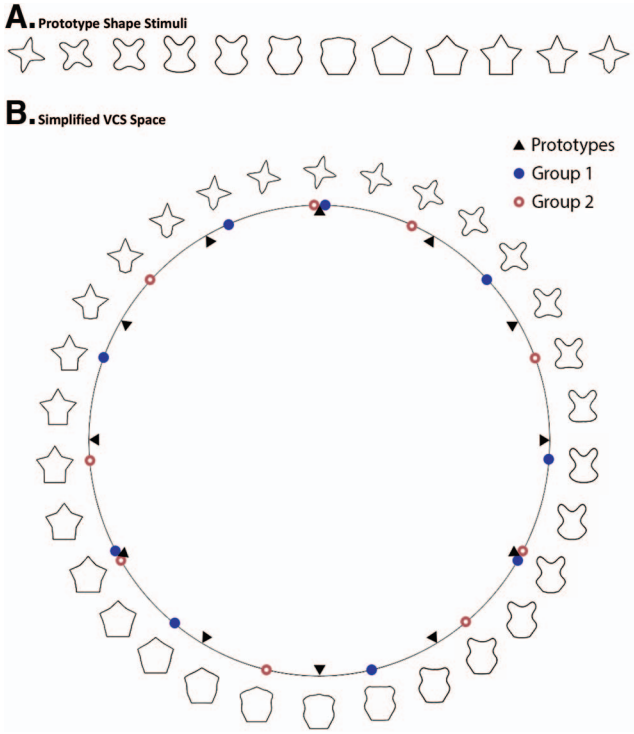

Figure 2. (A) The prototype shapes used to generate the stimulus space separated by 30 degrees of angular distance (positions denoted by triangles in Panel B). (B) Simplified Validated Circular Shape space with stimuli mapped to every 12 degrees of angular distance. The full circular stimulus space contained 360 stimuli, with a unique morphed shape mapped to each degree on the wheel. Morphs were obtained by blending the prototype shapes, the positions of which are denoted by black triangles. Closed blue denote shapes rated in Group 1, whereas open red denote shapes rated in Group 2. Three shapes were shared in Group 1 and 2, representing the anchors used to align the shape space reconstructions from each group (described in the main text under *Validation Procedure*). See the online article for the color version of this figure.

discarded when the similarity between shapes was excessively similar. In other cases, additional shapes may have been included in regions where shapes were more dissimilar than expected. Through the iterative correction of problematic shapes, MDS was used to create a data-driven circular space without the need to mathematically define the dimensions underlying the representation of visual form. Thus, VCS space was made to be perceptually uniform (Figure 1B), in contrast to other approaches that did not empirically collect similarity judgments (Salmela et al., 2010; Zhang & Luck, 2008). In Step 6, for the final validation iteration we quantified the exact relationship between angular distance and visual similarity using a *distance function*, mapping a single numerical similarity value onto each degree of VCS space. The creation of this distance function was based on previous work on circular color space (Schurgin et al., 2018).

We define the start of one validation "iteration" by the creation of a set of prototype shapes. There were seven iterations in total. For brevity, in the main text we report the methods and results of the seventh iteration that ensured VCS space was circular, as well as an overview of the experimental procedure. See the online supplemental material for details on the earlier iterations, including how prototype shapes were selected and the specific criterion for defining problematic shapes.

Participant Recruitment

Sixty-seven participants (M_{age} = 21.58 years, *SD* = 2.76 years, women = 48) were tested across all seven validation iterations, recruited from the undergraduate psychology student pool at the University of Toronto and from the community. Participants from the undergraduate student pool were compensated with course credit. Participants from the community were compensated $20 CAD for the final validation iteration and $10 CAD for the first throught sixth iterations. The final validation iteration required up to 90 min to complete, which included time for instructions, a practice session, the actual experiment, and debriefing. Earlier validation iterations contained fewer stimuli to be rated and required under an hour to complete. We recruited new individuals for each validation iteration. This study was approved by the University of Toronto Ethics Board: Protocol number 23778.

It was not possible to determine an a priori sample size because the quantitative measures of circularity were descriptive rather than inferential (Figure 3E). Instead, we developed VCS space over many iterations, whereby the stimulus space was successively replicated seven times. For example, in the sixth validation iteration (see Validation 6 in the online supplemental material), a single problematic region on the reconstructed shape space was identified. Fixing that single problematic region in the final validation iteration produced a circular shape space. The successive replication of VCS space over each iteration combined with a novel procedure involving the alignment of shape space across two independent groups (described in the *Validation Procedure* section) was intended to maximize the generalizability of our findings. Overall, the final validation iteration tested a sample size of 21 individuals (M_{age} = 22.52 years, *SD* = 4.14 years, women = 13).

Apparatus

The validation experiment was created in MATLAB using Psychtoolbox-3 (Kleiner, Brainard, & Pelli, 2007). All stimuli were displayed on the monitor of a Latitude 3460 Dell laptop with a resolution of 1,920 × 1,080 and a frame refresh rate of 60 Hz. The monitor was 12.18 in × 6.85 in wide. The distance from the monitor to the participant was approximately 50 cm. All shape stimuli were presented on top of a uniform white background, subtending approximately 3.44 degrees of visual angle. Participants responded to on-screen instructions using the keyboard keys.

Validation Procedure

Step 1: Designing prototype shapes. In the first validation iteration (see the online supplemental material), a set of 2D shape line drawings were created as prototypes. These first prototype shapes were designed to be visually distinct while controlling for the approximate size of each shape. As we were specifically interested in capturing visual similarity along a 2D circle, we did not explicitly control for any other lower or higher-order stimulus properties, although these properties may have been implicitly

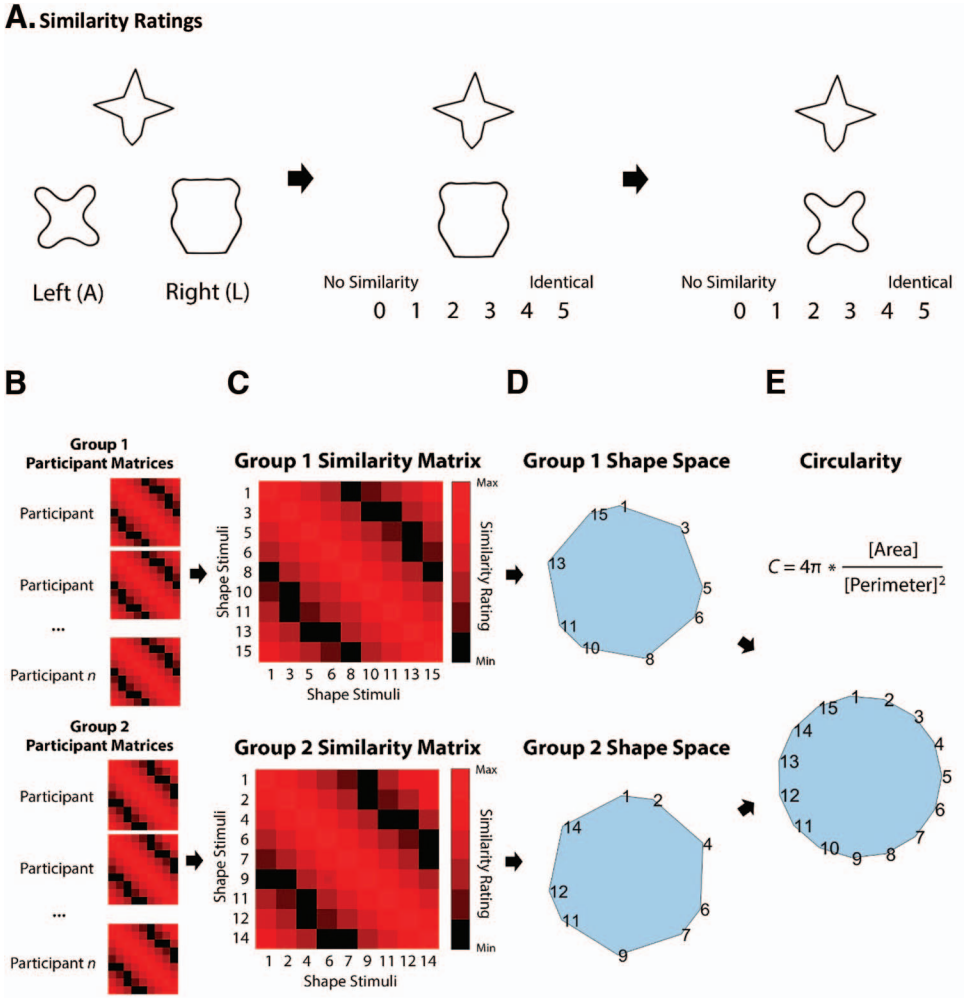

Figure 3. Similarity validation procedure using simulated data for illustrative purposes. (A) Participants were shown three shapes sampled from the set every trial, and judged which of the bottom shapes were more similar to the top one. After a response, participants rated the similarity between the top shape and bottom shapes. (B) The similarity judgments were averaged to create a similarity matrix for each participant. (C) All participant similarity matrices were then averaged to produce a similarity matrix for each group, whereby each cell represents the average similarity between two shapes sampled from the stimulus space. (D) Multidimensional scaling was used to reconstruct the subjective shape space from each group similarity matrix. (E) Last, the Group 1 and Group 2 shape spaces were aligned together to produce a single shape space. A quantitative circularity score characterized the extent to which the aligned subjective shape space was circular. See the online article for the color version of this figure.

controlled through the visual similarity judgments. See the *Discussion* section for the implications of the initial selection of these prototypes on the final shape space. Prototype shapes were then incrementally corrected across each validation iteration until no problematic shapes were present. In the final validation iteration, 12 prototype shapes (Figure 2A) were created by redesigning the problematic region from the previous validation iteration (see Validation 6 in the online supplemental material). Problematic shapes were manually redesigned using Photoshop, taking care to keep the change in similarity approximately uniform across all prototypes.

Step 2: Morphing. Neighboring pairs of prototype shapes were then morphed using SqirlzMorph (Xiberpix, 2008). If visual artifacts were observed as a result of morphing, Photoshop was used to manually smooth the artifacts. This morphing procedure generated a circular stimulus space of 360 unique shapes (Figure 2B) from a set of 12 initial prototypes (Figure 2A).

Fifteen shapes spaced equidistantly—every 24 degrees—on this stimulus space were selected for validation. Participants were randomly separated either into Group 1 (n = 11) or Group 2 (n = 10); each group rated six unique shapes in addition to three "anchor shapes" that were identical to both groups (see Figure 2B, shapes denoted by closed blue and open red). Critically, the stimuli selected for validation were different from the prototype shapes used to build the space, with the exception of the anchor shapes which were prototypes. These three anchor shapes were specifi-

cally selected to be maximally distinct from each other, estimated from the results of the previous validation iteration. We aligned the reconstructed spaces from the two groups by the anchor shapes (described in Step 4) based on the similarity ratings (described in Step 3). Importantly, not all validation iterations required the selection of anchor shapes, as not all validation iterations required alignment (see the online supplemental material).

Step 3: Similarity ratings. Participants were presented detailed instructions and completed a short practice version (five trials) of the task prior to the procedure. The nine shapes selected for each group (denoted by closed blue and open red in Figure 2B) formed the stimuli to be rated for that group. Every trial, one shape was displayed near the top of the screen and two shapes were displayed near the bottom left and bottom right of the screen (Figure 3A); 800 ms later, participants were then cued with text to select the shape on the bottom left ("A" key) or the bottom right ("L" key) that was most visually similar to the shape positioned at the top of the screen. This initial judgment phase in which triads were presented (Figure 3A) allowed observers to calibrate to the shapes being rated on a given trial. One thousand ms after a response, the shape on the top and one of the two bottom shapes were randomly paired together; 800 ms later, participants rated the similarity of the paired shapes with 0 being "*no similarity*" and 5 being "*identical.*" One thousand ms after a response, the top shape was displayed with the other bottom shape that had not been rated; 800 ms later, participants again rated the similarity of the paired shapes with 0 being "*no similarity*" and 5 being "*identical.*" After this last response, a screen appeared with the number of trials completed, and participants pressed the space key to begin the next trial. Importantly, short delays were included between the presentation of a shape and the presentation of the rating scale, so that participants studied the presented shapes rather than responding in a speeded way. We also emphasized to participants that they should use the entire rating scale during the experiment.

Over the course of the experiment, shapes were randomly sampled during the first triad of every trial such that relative to each individual shape in the set, all possible combinations of shape pairs were sampled. More specifically, participants made pairwise ratings between each shape relative to each other shape 14 times (e.g., Shape 1 was rated relative to Shape 2 in 14 different instances; of these 14 instances, Shape 1 was presented at the top of the initial triad seven times and at the bottom left or right of the initial triad seven times). Each of the nine shapes was also rated on two trials relative to itself (e.g., Shape 1 with Shape 1). This created the diagonal in the similarity matrices (Figure 3B and 3C). These rules generated a list of three shapes every trial, and the presentation order of these trials were randomized. For these reasons, the final validation iteration required 270 trials. Earlier validation iterations required less trials (see the online supplemental material).

All pairwise ratings involving the same two shapes were averaged (e.g., the similarity values between Shape 1 and Shape 2 were averaged across all instances shown in the initial triad). These mean scores take into account the overall similarity of the set and were represented within a similarity matrix for each participant (Figure 3B). These participant similarity matrices were then averaged across participants to produce a single similarity matrix for each group (Figure 3C). All participant and group matrices were symmetrical due to the averaging procedure. This within-subject procedure was expected to increase power, reduce error, and allow MDS to recreate subjective space with greater precision. Indeed, the high number of trials ($n = 14$) for each pairwise rating between the same two shapes ensured high reliability of the visual similarity estimate between shapes on the stimulus space.

Step 4: Reconstructing shape space. From the averaged similarity matrix in each group (Figure 3C), shape space was reconstructed with MDS (Figure 3D) using the *mdscale* function in MATLAB. The anchor shapes (i.e., shapes that were the same in each group) were then used to align the reconstructed shape space from each group together (Figure 3E). Here, we used two separate alignment functions: Procrustes transformation (Figure 4A) and affine transformation (Figure 4B). Procrustes transformation preserves the relational structure of the space in both groups, which may result in imperfect alignment. In contrast, affine transformation includes an additional "skew" step and can perfectly align the two group shape spaces by the three anchor points but may distort the relational structure of one of the spaces. As the affine transformation may alter the relational structure of one group space (Figure 4B), we visually compared the solutions obtained from the Procrustes and the affine transformations. Furthermore, only the affine aligned shape space could be used to quantitatively determine whether the final validation iteration was circular, as the Procrustes transformation does not perfectly align the group spaces (see *Step 5:* "Assessing Circularity" section).

We could not collect ratings for all 360 shapes from VCS space due to the exorbitant number of trials required for pairwise similarity judgments (64,620 trials just to collect a single rating for all pairwise combinations of 360 shapes). Researchers have previously decreased the number of trials needed by using a spatial similarity method (Kriegeskorte & Mur, 2012), in which participants "drag-and-drop" stimuli to locations on a computer screen. In this method, observers use the spatial proximity of items as an index of visual similarity. However, because our goal was to develop a particular spatial configuration (i.e., a circle), we did not want to bias participants into using a spatial similarity method which may unintentionally lead to circular configurations (Verheyen, Voorspoels, Vanpaemel, & Storms, 2016). Our novel procedure in which two independent groups each rated six unique shapes + three anchor shapes was instead used to infer the overall relational structure of VCS space. This method provides the most powerful demonstration that the space was indeed circular, because a circular space could have only been reconstructed across groups if visual similarity changed uniformly and incrementally across the entire stimulus space.

Statistical Analysis

Step 5: Assessing circularity. It is standard practice for experimenters to qualitatively interpret reconstructed space, as MDS is a descriptive analysis (for examples of previous applications of MDS in the cognitive sciences, see Hout, Goldinger et al., 2013; Hout, Papesh, & Goldinger, 2013; Hout et al., 2016; Shepard, 1980). In addition to this qualitative assessment, we added a novel quantitative approach to assess whether or not a reconstructed shape space was circular. Circularity was defined using a simple mathematical ratio that captures the relationship between the area and perimeter of a spatial configuration. More specifically, the circle is the spatial configuration with the largest area relative to

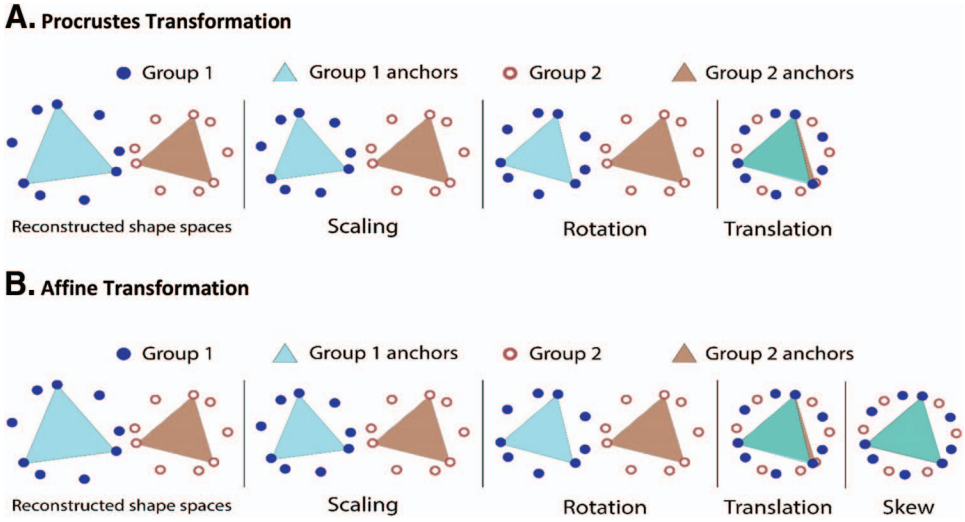

Figure 4. Visualization of the alignment procedure, whereby the transformation order of steps is simplified and the expected positional differences between spaces is exaggerated for illustrative purposes. First, multidimensional scaling was used to reconstruct a separate shape space from each group similarity matrix. Separate alignment functions were then applied to the two shape spaces. Linear transformations are first determined for the anchor shapes, shown as a triangle, then applied to the rest of the space. (A) Procrustes transformation includes scaling, rotation, and translation, which preserves the relational structure of both spaces but can lead to imperfect alignment. (B) Affine transformation includes scaling, rotation, translation, and skew, which can distort the relational structure of one of the group shape spaces but will perfectly align both groups together. See the online article for the color version of this figure.

perimeter in the plane (see isoperimetric inequality; Osserman, 1978):

$$Circularity\ \ (C) = \ \ 4\pi \times \frac{[Area]}{[Perimeter]^2}$$

To calculate C, borders were drawn between the projected coordinates of each shape in the aligned shape space (Figure 3E), following the relational structure of the original stimulus space (Figure 2B). For example, if the reconstructed position of Shape 1 was at 1 degree on the stimulus space, Shape 2 at 25 degrees, and Shape 3 at 49 degrees, then a border was drawn from Shape 1 to Shape 2 to Shape 3 (and so forth, with the final shape connected back to Shape 1). Area and perimeter were then calculated to determine a value of C (Figure 3E). A space that is a perfect circle will have a C value equal to 1.0. As a space is increasingly less circular, C will approach 0.0. To complement this quantitative circularity score, we qualitatively assessed whether the positioning of the vertices within the reconstructed shape space approximately matched the vertices of the original stimulus space. For every validation iteration, a reconstructed shape space was defined quantitatively as sufficiently circular when C exceeded 0.90 and qualitatively as sufficiently circular when the relative positions of the vertices approximately matched the original shape space. $C = 0.90$ was selected as the threshold for circularity as this value indicates a geometry that is qualitatively close to a perfect circle, confirmed through simulations (commented code available on the Open Science Framework: https://osf.io/d9gyf/). A detailed description of these simulations and pictorial examples are available in *Circularity Simulations* in the online supplemental material. Also see Figure 5 for examples of how the measure of C tracked circularity from the first validation iteration to the final validation iteration.

C was calculated specifically for the affine aligned shape space (Figure 4B). We used the affine aligned shape space to determine C rather than the Procrustes aligned shape space, because Procrustes transform does not always perfectly align the two group shape spaces together (Figure 4A). However, because the affine alignment procedure may distort the relational structure of one group shape space (Figure 4B), we conducted both Procrustes and affine transformations and visually compared the solutions. Permutation testing was conducted to determine whether the C value for the affine aligned shape space could have been obtained by chance. The shape labels of each participant matrix were shuffled to form a scrambled version of Figure 3B. These null participant matrices were averaged together to produce a null group similarity matrix (a scrambled version of Figure 3C). Null MDS coordinates were then projected from each null group similarity matrix, forming a null reconstructed space for each group. These null shape spaces were aligned together to produce a null affine aligned shape space. A null C score then determined the circularity of this null affine aligned shape space. This process was repeated 10,000 times to generate a null distribution of C scores. Statistical significance was defined as probability $p < 0.05$ for the observed C score relative to the null distribution of C scores. Critically, the observed C value derived from the reconstructed subjective space gives information regarding circularity, whereas the p value obtained from permutation testing gives information regarding whether the subjective space could be formed by chance. A subjective shape could be noncircular (e.g., $C = 0.75$, see Figure 5), yet could be statistically significant (e.g., $p < 0.05$) because participants may be homogenous in how they perceived a stimulus space.

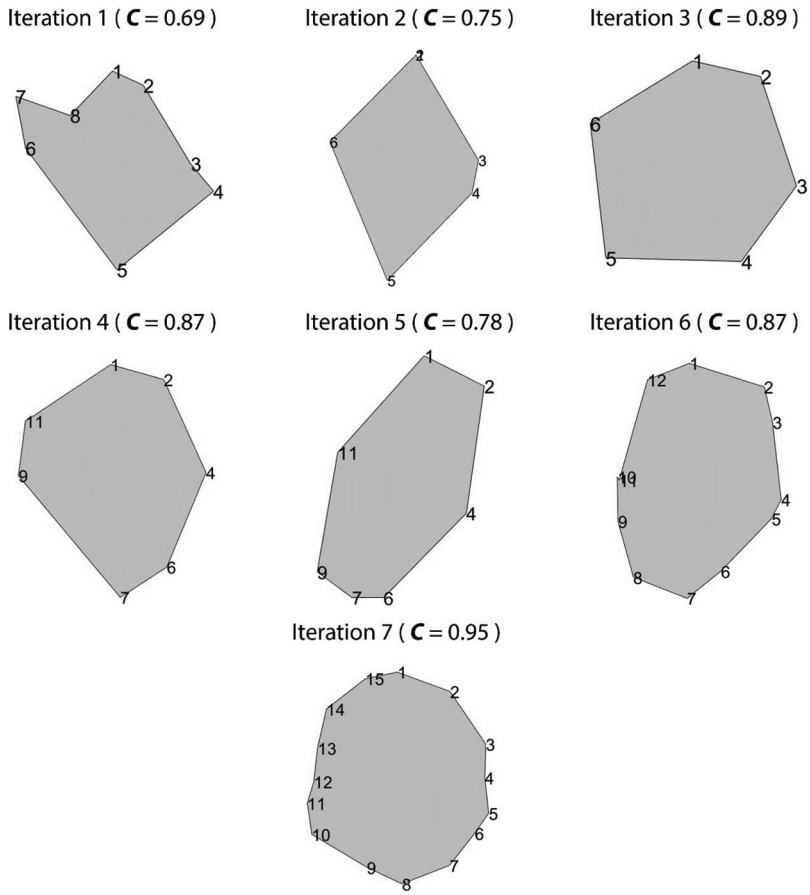

Figure 5. *C* was calculated for each validation iteration (see the online supplemental material for detailed results). All validation iterations were statistically significant using permutation testing. Numbers represent the position of each shape from the associated stimulus space.

We also examined the uniformity of individual shape spaces by calculating a *homogeneity score* representing the overall consistency between all the similarity judgments made for a given validation iteration. To calculate this score, each participant matrix (Figure 3B) was correlated with every other participant matrix. As participant matrices were symmetrical (see *Step 3: Similarity Ratings* section), only the upper triangle of each participant matrix excluding the diagonal was correlated to each other. This created a new matrix with elements containing the correlation between each participant to every other participant. We first normalized these correlations by transforming to Fisher's *z* (Corey, Dunlap, & Burke, 1998). These *z* values were averaged then transformed back into a correlation value to produce a single score representing the degree to which individuals homogeneously perceived a shape space.

Permutation testing was conducted to compute the likelihood of observing the homogeneity score by chance. The labels of each participant matrix (Figure 3B) were shuffled and the upper triangle of these matrices were correlated to each other, forming a null correlation matrix. We then averaged the normalized correlations in the upper triangle of the null between-participants correlation matrix to produce a null homogeneity score. This procedure was repeated 10,000 times to produce a null distribution of homogeneity scores. Statistical significance was defined as probability $p < 0.05$ for the observed homogeneity score relative to the null distribution of homogeneity scores.

Step 6: Distance function. Similarity can be considered in two ways for a circular space (Figure 1B). First, an ideal circular space is perceptually uniform, meaning that items sampled from any distance are about as similar as any other items sampled from that same distance. Second, the magnitude of similarity can be approximated by angular distance, meaning that items closer in angular distance are more similar than items further in angular distance. The circularity value (Figure 3E) gives information regarding the degree to which the shape space is perceptually uniform. However, the circularity value does not give information regarding the magnitude of the numerical change in similarity from one shape to the next.

To determine if angular distance is an approximation of visual similarity, we combined a quantitative and qualitative approach. Quantitatively, a function was used to predict the collected similarity ratings using the angular distance of shapes positioned on the stimulus space, akin to a regression analysis predicting visual similarity from angular distance. This distance function mathematically describes the relationship between angular distance and visual similarity on VCS space (see *Results* for a step-by-step

description). In this way, a numerical similarity value was obtained for each possible pairing of the 360 shapes in VCS space, even though ratings were only collected for 15 shapes (Figure 2B). Qualitatively, we examined the change in visual similarity with respect to angular distance in each group similarity matrix (Figure 3C). If angular distance approximated visual similarity, then shapes closer in angular distance should be associated with a higher similarity rating than shapes further in angular distance.

Summary of analyses. We computed the following set of measurements: (a) *C*, representing the circularity of the affine aligned shape space; (b) the *homogeneity score*, representing the mean correlation between all participant similarity judgments, and in the final validation iteration; (c) a *distance function* quantified the relationship between angular distance and visual similarity.

Two types of similarity on VCS space were examined (Figure 1B): whether the space was perceptually uniform and whether angular distance approximated visual similarity. First, a reconstructed shape space was defined as sufficiently circular (i.e., perceptually uniform) when *C* exceeded 0.90 and when qualitatively, the relative positions of all vertices of the reconstructed shape space tended to match the original stimulus space. Second, if angular distance approximated visual similarity, then shapes closer in angular distance should be more similar than shapes further away.

Results

Validation Iterations 1–6

Circularity. Seven validation iterations were required to exceed a *C* score of 0.90 (Figure 6; the online supplemental material). We found that the first validation iteration was not circular ($C = 0.69$), suggesting that stimulus spaces arranged by experimenters without explicitly collecting similarity judgments may not match visual similarity. All *C* scores (Figure 6A) were significantly different from what would be expected by chance alone (at or below $p < 0.01$ using permutation testing; see *Step 5:* "Assessing Circularity" section for a description of the analysis). This suggests that the reconstructed shape space within each iteration could not have been obtained by chance, but rather reflects the degree to which the stimulus space is perceptually uniform.

Homogeneity score. The mean correlation between participant similarity judgments was consistently very high across all validation iterations (all homogeneity scores were statistically significant using permutation testing at $p < 0.0001$; Figure 6B). Overall, this result suggests that individuals were very similar to each other in their representation of the stimulus space across validation iterations, even when the stimulus space in a specific validation iteration was not circular.

Final Validation Iteration

Circularity. In the seventh and final validation iteration, *C* of the affine aligned shape space was 0.95 ($p < 0.0001$ using permutation testing), suggesting that it was circular (Figure 7). Qualitatively, the positions of shapes on both the Procrustes (Figure 7B) and affine aligned (Figure 7C) shape space approximately matched the positions of shapes sampled from VCS space. These results confirmed that VCS space was circular, as the shapes to be rated in each group were sampled from arbitrary positions on the original stimulus space. For detailed group results, see Validation 7 in the online supplemental material.

Complimenting the alignment procedure, when the Group 2 similarity matrix was overlaid with the Group 1 similarity matrix (Figure 8), a striking trend could be observed. Angular distance approximated (though was not identical to) visual similarity: visual similarity tended to decrease as angular distance increased. For example, Shape 1 and Shape 2 were separated by 24 degrees on VCS space and were associated with a similarity value of 3.8 (see the second element of the first row on Figure 8). Increasing the

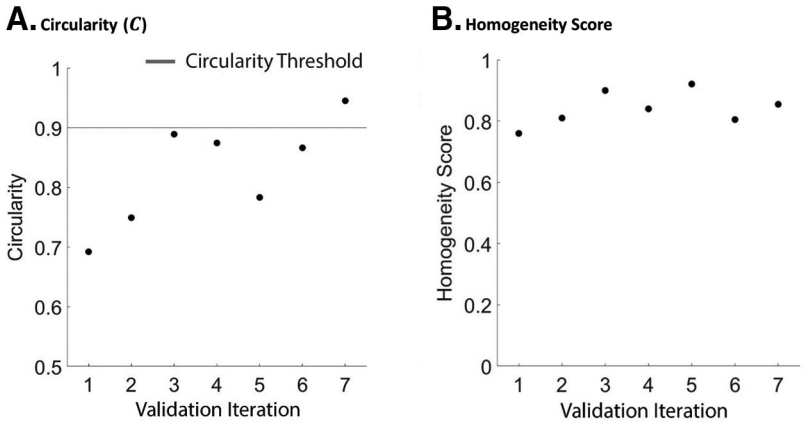

Figure 6. Overall results across validation iterations. (A) *C* by validation iteration, representing the degree to which each stimulus space was perceptually uniform. Higher values reflect a space that is closer to a perfect circle, meaning a space that is more perceptually uniform. (B) Homogeneity scores by validation iteration, reflecting the mean correlation between participant similarity judgments. The homogeneity score determined for each group was averaged to produce a single value for a given validation iteration in the plot above. These results suggest that even if a stimulus space in a validation iteration was not circular, participants were homogeneous in how they perceived shape similarity.

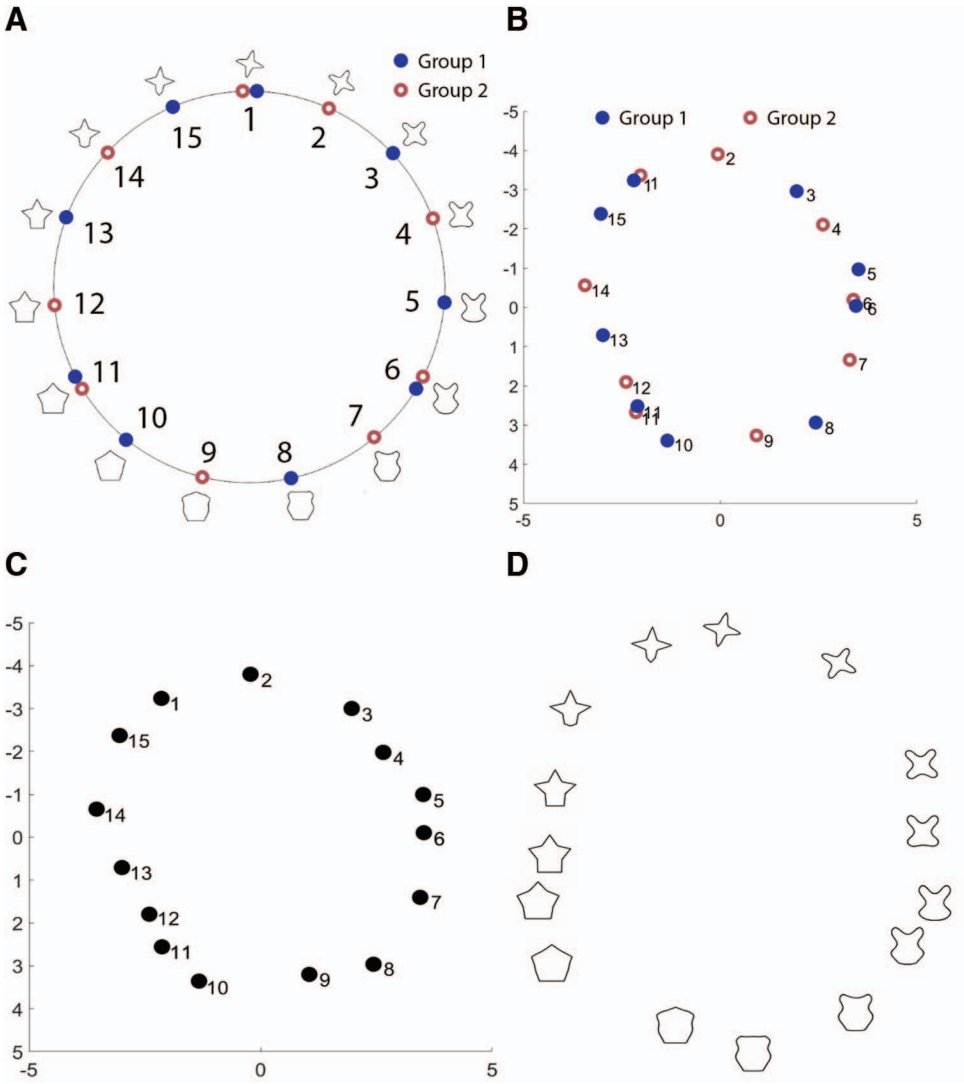

Figure 7. Results of the final validation iteration. Numbers represent the sequential position of the rated shapes sampled from the Validated Circular Shape (VCS) space (e.g., each rated shape was 24 degrees apart, so Shape 1 would be at 1 degree, Shape 2 at 25 degrees, Shape 3 at 49 degrees, and so on). (A) Simplified VCS space labeled with the shapes rated during the final validation iteration. (B) Procrustes alignment of Group 1 (closed blue) and Group 2 (open red). (C) Affine alignment between Group 1 and 2. Both alignment functions were highly similar and both resulted in circular reconstructions (D). The final shape space reconstructed by affine transformation on the multidimensional scaling solutions from Group 1 and 2. See the online article for the color version of this figure.

angular distance between shapes by another 24 degrees and comparing Shapes 1 and 3 decreased the observed similarity rating to a value of 3 (see the third element of the first row on Figure 8). Importantly, this matrix was created from combining the similarity ratings *across groups* with no adjustment whatsoever. That is, we overlaid the similarity matrices from each group (see Validation 7 in the online supplemental material) into a single matrix without interpolation across groups, further confirming that the change in visual similarity across VCS space was uniform.

Homogeneity score. The homogeneity score was very high in both groups (Group 1 = 0.87, Group 2 = 0.86), suggesting that participant similarity judgments were highly correlated to each other (Figure 6B). The observed correlation across participants could not be based on chance alone, as both homogeneity scores were statistically significant at $p < 0.0001$ using permutation testing.

Distance function. We quantified the exact relationship between angular distance and visual similarity on VCS space, inspired by previous work on a distance function for circular color space (Schurgin et al., 2018). Using the collected similarity judgments across both groups (Figure 8), the visual similarity of each shape relative to the set was plotted by degrees on VCS space. This is shown on Figure 9A, where every 24 degrees reflects the similarity value of one shape relative to every other shape in the

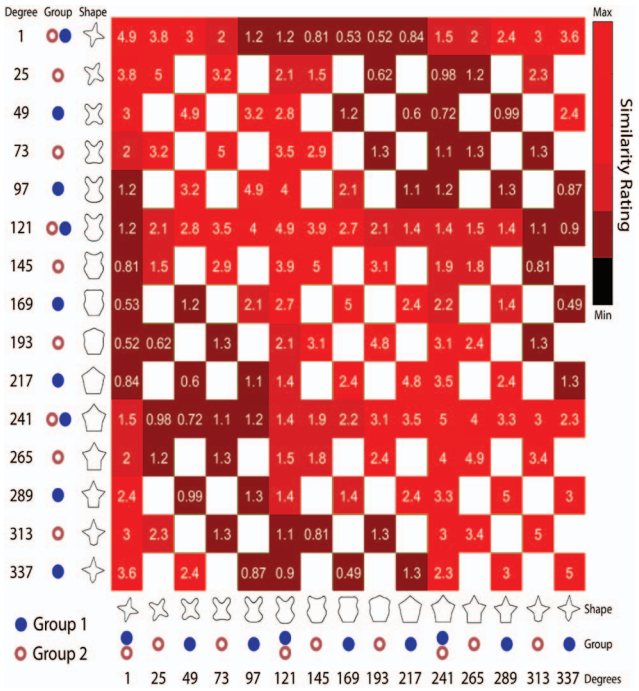

Figure 8. The similarity matrix for Group 2 was simply combined with the similarity matrix for Group 1. Elements with a value in both Group 1 and Group 2 were averaged together. Blank elements refer to pairs of shapes that did not have a similarity rating as they were in distinct groups. Each element refers to the averaged similarity rating across all participants, bounded from 0 (*no similarity*) to 5 (*identical*). The *x*- and y-axis include the rated shapes, the group, and the position on the Validated Circular Shape space (Figure 2b) from which the shape was sampled. Here, we see a striking trend in similarity across groups, whereby shapes closer in angular distance were rated more similarly compared to shapes further in angular distance. See the online article for the color version of this figure.

set. For example, the similarity between Shape 1 rated with itself is plotted at 0 degrees, Shape 1 rated with Shape 2 is plotted at 24 degrees, Shape 1 rated with Shape 3 is plotted at 48 degrees, and so forth. Likewise, the similarity between Shape 2 rated with itself is plotted at 0 degrees, Shape 2 rated with Shape 3 is plotted at 24 degrees, Shape 2 rated with Shape 4 is plotted at 48 degrees, and so forth until all similarity values from Figure 8 are plotted on Figure 9A.

These collected similarity ratings were averaged and then re-plotted by angular distance (Figure 9B). More specifically, the angular distance between Shape 1 relative to Shape 2 as well as Shape 1 relative to Shape 15 is 24 degrees' distance (because shapes are mapped along 360 degrees of a circle). All instances between pairs of shapes with equivalent angular distances were averaged to obtain a single similarity value at every 24 degrees' distance. To predict a similarity value for each degree on VCS space given our observed similarity ratings, a nonlinear exponential function successfully fit the relationship between visual similarity and angular distance ($R^2 = 0.998$; Figure 9B). This nonlinear function was normalized to create the line in Figure 9C. Normalization converted the *y*-axis of this function from our similarity rating scale (0–5) to a percentage scale (0–100%). Taken together, this distance function predicted a numerical similarity value—a percentage match in visual similarity—between any two shapes sampled from VCS space. Angular distance was an approximation of visual similarity, as the visual similarity between two shapes incrementally decreased as angular distance increased (Figure 9C).

Discussion

We provide and characterize the VCS space, the first perceptually uniform shape space whereby the angular distance between 360 shapes mapped on a 2D circle is a proxy for visual similarity (available on the Open Science Framework: https://osf.io/d9gyf/). To achieve this property, VCS space was developed across a series of seven validation iterations. In the final validation iteration, MDS reconstructions from the similarity ratings of two separate groups were aligned to recreate the original circular stimulus space. A quantitative measure of circularity then precisely captured the representational geometry of the reconstructed stimulus space, to our best knowledge the first application of isoperimetric inequality in the domain of similarity data. VCS space is comparable to a "color wheel" built from CIELAB color space (Figure 1), whereby the distances between stimuli are known to approximate the way in which human observers perceive color similarity (McDermott & Webster, 2012; Pointer, 1981; Robertson, 1977).

Experimenters using VCS space may consider similarity in two ways. VCS space is perceptually uniform, meaning that shapes separated by any distance are about as similar as any other shapes separated by the same distance. By sampling stimuli from equidistant angular positions on VCS space, the variability in similarity from one shape to the next is consistent across the set. In this way, the experimenter could use VCS space alone or in conjunction with color space so that the similarity of multiple features within an object can be empirically manipulated (Figure 10A). The second way to consider similarity on VCS space is with respect to *magnitude*, meaning that shapes closer in angular distance tend to be more similar than shapes further in angular distance. Though our distance function revealed that angular distance very closely tracked visual similarity, angular distance was not perfectly analogous to the magnitude of visual similarity between items (Figure 8 and 9B). If the magnitude of similarity must be quantified with numerical precision, the researcher may consider using our distance function (also available on the Open Science Framework: https://osf.io/d9gyf/; see Figure 9C). For example, in Figure 10B, each shape was sampled using the distance function so that the magnitude of visual similarity changed incrementally by 20%. Depending on the particular research question, experimenters using VCS space may need to decide which of these properties should be emphasized for stimulus selection. For example, if the experimenter wishes to equate the variation in visual similarity, then sampling stimuli on the basis of angular distance will be sufficient (i.e., the perceptually uniform property). However, if the experimenter desires an exact numerical similarity value between stimuli (i.e., the magnitude property), then experimenters may wish to use our distance function to sample shapes (Figure 9 and 10). Importantly, the distinction between the perceptually uniform property and the magnitude of visual similarity on circular space has been at the center of an emerging debate in the memory literature (Schurgin et al., 2018). This debate focuses on the question of whether memory errors on certain tasks (e.g., continuous retrieval task) using circular space can be better described in

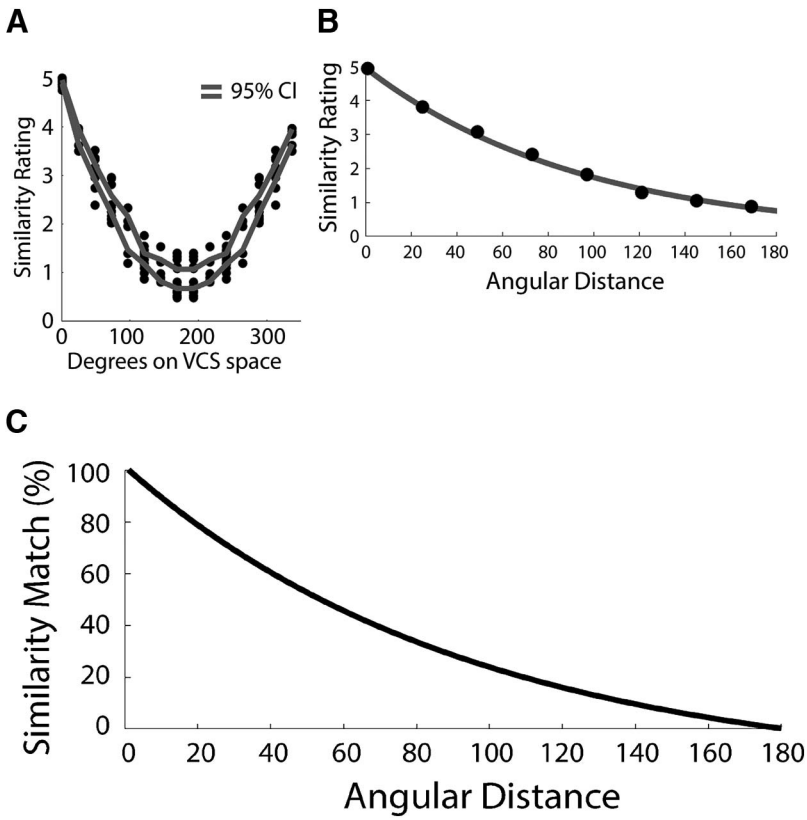

Figure 9. Validated Circular Shape (VCS) space distance function. (A) Relative to each rated shape, all similarity judgments from Figure 8 were replotted as a function of degrees on VCS space. Error bars reflect the 95% confidence interval for the mean similarity rating as a function of degrees on VCS space. (B) Average visual similarity as a function of angular distance. Angular distance approximated visual similarity, as a nonlinear exponential function ($R^2 = 0.998$) well predicted the relationship between angular distance and the observed similarity ratings. (C) The nonlinear exponential function was normalized to directly compare between shapes along a percentage scale, bounded by 100%, representing a perfect match in similarity, and 0%, representing maximal dissimilarity with respect to the shape space.

terms of angular distance which approximates the magnitude of similarity (Ma et al., 2014), or whether such errors are better described by the magnitude of similarity between a studied and reconstructed memory (see Figure 1B; Schurgin et al., 2018). For these reasons, future experiments using VCS space can examine the influence of incorporating the magnitude of similarity on memory errors in a continuous retrieval task (e.g., by using our distance function, Figure 9; Ma et al., 2014; Schurgin et al., 2018; Zhang & Luck, 2008).

VCS space is very precisely characterized in terms of the change in visual similarity along a 2D circle, comparable to the way similarity changes around circular color space. However, there are also several differences between our circular shape space compared to color space. Perceptually uniform color spaces span the complete range of trichromatic color vision (McDermott & Webster, 2012), whereas our shape space was necessarily constrained in scope due to limited number of prototype shapes used to develop VCS space. From iteration to iteration we prioritized improving how visual similarity was captured along a circle (Figure 5), rather than controlling for differences in lower-level shape properties such as curvature (Bell et al., 2010; Loffler, 2008; Wilson & Wilkinson, 2015), complexity (Brincat & Connor, 2004), or symmetry (Apthorp & Bell, 2015), or higher-level shape properties such as prototypicality (Feldman, 2000), likability (Bar & Neta, 2006), or processing fluency (Reber, Schwarz, & Winkielman, 2004). For these reasons, each exact dimension underlying the circular nature of VCS space is not known, nor do we know whether such dimensions on VCS space are integral or separable (Drucker & Aguirre, 2009; Drucker, Kerr, & Aguirre, 2009; Garner & Felfoldy, 1970; Grau & Kemler Nelson, 1988; Kemler Nelson, 1993; Offenbach, 1990). Depending on the specific research question, experimenters may need to evaluate how VCS space differs across multiple dimensions to either account for these dimensions or determine what aspects of each dimension may be critical drivers for the phenomenon VCS space is used to research.

Nevertheless, the way in which visual similarity is captured along VCS space (Figure 1B and Figure 10) can be usefully adapted to examine theoretical questions in a variety of domains. For example, we used VCS space to replicate a memory effect previously demonstrated using circular color space (Sun, Fidalgo, et al., 2017). VCS space was used to quantify the visual similarity of distracting information (see Experiment 2 in Li, Liang, Lee, &

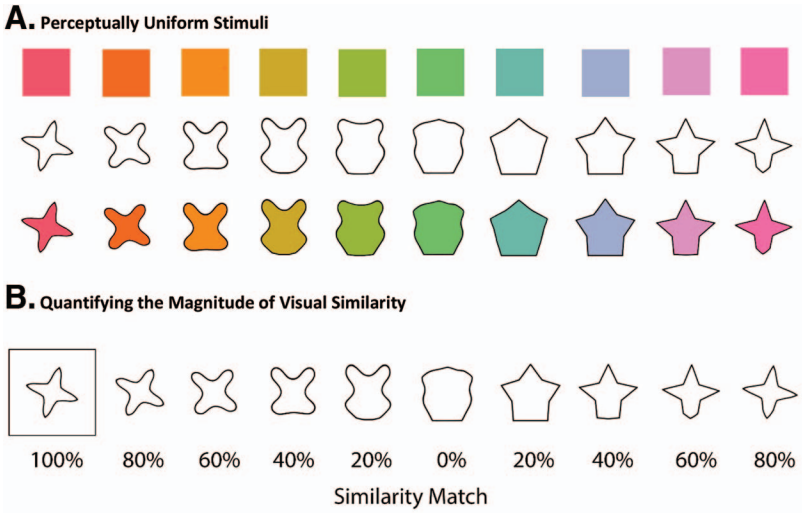

Figure 10. (A) Example of how the perceptually uniform property of Validated Circular Shape (VCS) space can be used in an experiment. Colors sampled from equidistant positions on CIELAB space (on a circle centered around $L = 70$, $a = 20$, $b = 38$, with radius = 60 units) and shapes sampled from equidistant positions on VCS space can be used to create objects with multiple features that are well-controlled in subjective variability. (B) The magnitude of visual similarity is approximated by angular distance on VCS space. To quantify the magnitude of visual similarity with numerical precision, we used our distance function to sample shapes. Each shape shown above differs by a 20% match in visual similarity relative to the shape displayed in the box. See the online article for the color version of this figure.

Barense, 2019; Li, Fidalgo, Liang, Lee, & Barense, 2018). Memory for target shapes were then tested after participants viewed either dissimilar or similar interference. We found robust interference effects that were consistent for both shape and color (Sun, Fidalgo, et al., 2017). Dissimilar interference disrupted both fine- and coarse-grained information, rendering the memory inaccessible. In contrast, similar interference disrupted fine-grained but increased the reliance on coarse-grained information, rendering the memory blurred. These results provide converging evidence for a set of generalizable rules regarding how the nature of interference influences memory, and also suggests that visual similarity on VCS space influences memory in a manner comparable to circular color space.

The neural mechanisms and principles by which shape is processed by the visual system is an currently active area of research (Bell et al., 2010; Cacciamani et al., 2015; Haushofer et al., 2008; Pasupathy et al., 2018; Peirce, 2015; Salmela et al., 2016; Sanguinetti et al., 2014). Here, the successful creation of VCS space directly implies the existence of a fundamental shape space coded by the visual system. This conclusion is additionally supported by the high homogeneity scores across each validation iteration (Figure 6C), suggesting that participants were highly correlated in how they perceived a stimulus space, even when a given stimulus space was not circular. Researchers have previously proposed that neurons sensitive to curvature may be important for processing visual form, with resultant models based on curvature detecting units (Bell et al., 2010; Gallant et al., 1993; Gallant, Connor, Rakshit, Lewis, & Van Essen, 1996; Loffler, 2008; Pasupathy, 2006; Pasupathy & Connor, 2002; Peterson & Gibson, 1994; Salmela et al., 2016; Schmidtmann & Fruend, 2019; Wilson & Wilkinson, 2015). One future direction of investigation may be to determine whether existing shape models can describe the circular organization of VCS space, because a successful model of shape representation should be able to explain why VCS space is circular at the level of the set (i.e., the perceptually uniform property) and why angular distance approximates the magnitude of visual similarity. For these reasons, understanding and characterizing the dimensions of VCS space may offer novel insight into how humans represent shape.

Another direction of investigation may involve neuroimaging to examine whether the circular organization of VCS space is reflected in patterns of neural activity. Akin to how color representations in V4 and VO1 are organized in a way similar to subjective color space (Brouwer & Heeger, 2009), and object representations in the inferior temporal cortex are organized in a way similar to subjective semantic space (Charest et al., 2014), neural representation of visual form may follow a similar organization to subjective shape space. One potential candidate is LOC, known to be important for shape processing (Drucker & Aguirre, 2009; Drucker et al., 2009; Grill-Spector, Kourtzi, & Kanwisher, 2001; Haushofer et al., 2008; Kourtzi & Kanwisher, 2000; Op de Beeck, Torfs, & Wagemans, 2008). In particular, the well-characterized nature of VCS space can be usefully combined with multivariate analyses which necessitate quantitative measures of similarity (e.g., see representational similarity analysis, Kriegeskorte et al., 2008; also see inverted encoding models, Brouwer & Heeger, 2009; Gardner & Liu, 2019; Kok & Turk-Browne, 2018; Sprague et al., 2018). Presently, it is common practice to select or create stimuli for behavioral and neuroimaging experiments based on experimenter intuition (e.g., word lists, scenes, faces, objects, complex sound stimuli), such that these stimuli can vary on many different unknown integral or separable dimensions. We believe that VCS space is an improvement on this practice, as visual similarity was

precisely quantified along a circular continuum (i.e., the perceptually uniform property and the magnitude property; Figure 1B). For these reasons, VCS space may be a useful stimulus space for studying neural representations in future work.

Qualitatively, one organizing dimension underlying VCS space is likely the curvature along the contour of each shape (Gallant et al., 1993; Pasupathy et al., 2018; Pasupathy & Connor, 2002; Ponce, Hartmann, & Livingstone, 2017; Yue, Pourladian, Tootell, & Ungerleider, 2014). Observation of the horizontal axis on VCS space seems to suggest a division organized by the degree to which a shape possesses sharp as opposed to curved edges (Figure 2B). Supporting this observation, previous studies of shape-sensitive cortex in nonhuman primates have found neurons with selective tuning to line curvature irrespective of size or orientation (El-Shamayleh & Pasupathy, 2016; Nandy, Sharpee, Reynolds, & Mitchell, 2013; Pasupathy, 2006; Yue et al., 2014). Interestingly, a curved-sharp shape dimension also seems to map onto crossmodal correspondences between shape and other sensory modalities (Velasco, Woods, Petit, Cheok, & Spence, 2016). There is a ubiquitous tendency for curved shapes to be rated as possessing softer, sweeter, and more pleasant characteristics compared to sharply angled shapes (Hanson-Vaux, Crisinel, & Spence, 2013; Spence & Ngo, 2012; Turoman, Velasco, Chen, Huang, & Spence, 2018). For example, whereas curved shapes are systematically rated to taste like vanilla and mint, sharply angled shapes are systematically rated to taste like pepper and cheese (Seo et al., 2010). The crossmodal correspondence between curved and sharply angled shapes to the other senses may perhaps reflect a neural division of curvature in the cortex and is an intriguing line of future investigation. That is, clusters of curvature sensitive neurons may have differential connectivity to other sensory cortices, a conjecture supported by evidence of discrete curvature-processing sites in the visual cortex (Yue et al., 2014). However, further experiments are needed to empirically determine if the dimensions underlying the circular nature of VCS space are applicable to the study of crossmodal correspondences.

Importantly, as it was not possible to collect pairwise similarity judgments for all 360 shapes on VCS space (64,620 trials just to collect a single rating for all pairwise combinations of 360 shapes), we developed a novel procedure involving shape space alignment between two independent groups of participants (Figure 3E and 4). The only way that alignment between two independent groups could reconstruct the overall shape space is if visual shape similarity changed incrementally and uniformly on VCS space across observers. Indeed, successful alignment confirmed the creation of a circular shape space (Figure 7), overcoming both the limited sample size and the limited number of shapes rated from VCS space in each group (six unique shapes + three anchors; see Figure 7 and 8). Future experiments can increase the number of shapes sampled from VCS space for validation and explore the potential strengths and weaknesses of our validation approach. Nevertheless, this novel methodology may be useful for researchers interested in developing and characterizing new stimulus spaces validated on properties other than visual similarity and for features beyond shape. In our method, MDS visualized the representational geometry of the stimulus space, and then this space was iteratively adjusted using the information observed from the collected similarity judgments. Throughout this process, a quantitative score based on isoperimetric inequality (Fusco, 2015; Osserman, 1978) determined the extent to which each iteration of VCS space was circular (see *Step 5:* "Assessing Circularity" section). Critically, formulas based on isoperimetric inequalities can be generated for many other types of spatial configurations. For example, if an experimenter wished to create a spherical 3D stimulus space, a quantitative score can capture the ratio between volume and surface area (i.e., the sphere is the configuration with the largest volume relative to surface area in three dimensions; Kesavan, 2002; Osserman, 1978). Moreover, isoperimetric inequalities exist for polygons in two dimensions such as squares and triangles (i.e., the equilateral triangle is the polygon of three edges with greatest area relative to perimeter), as well as complex configurations of very high dimensionality (Fusco, 2015; Kesavan, 2002). Quantitative scores can be useful in determining the degree to which a stimulus space matches a desired configuration, though considerable time and resources may be required to validate geometries of high dimensionality.

Taken together, VCS space can be extended broadly as a resource to any experimenter who wishes to use shapes whose visual similarity has been validated. For example, experimenters can use VCS space for stimulus selection (e.g., by selecting shapes every 36 degrees' distance to create a set of 10 unique shapes for each participant; Figure 10A), greatly simplifying the stimulus design process. Experimenters can additionally use the properties of VCS space to gain precise control over the variation and the amount of visual similarity of shapes sampled into multiple experimental conditions (Figure 1B and Figure 10). For these reasons, VCS space may be useful in any research domain which commonly uses shape stimuli, including the study of attention (e.g., Connor, Egeth, & Yantis, 2004), categorization (e.g., Jiang et al., 2007), crossmodal correspondences (e.g., Chen, Huang, Woods, & Spence, 2016), ensemble perception (e.g., Whitney & Yamanashi Leib, 2018), shape symbolism (e.g., Spence & Ngo, 2012), short- and long-term memory (e.g., Fukuda, Awh, & Vogel, 2010; Ma et al., 2014; Sun, Fidalgo, et al., 2017; Yassa & Stark, 2011; Yonelinas, 2013), and statistical learning (e.g., Abla & Okanoya, 2009). Moreover, the circular nature of VCS space can be directly extended for use with mixture models to capture both the resolution of memories and the probability of outlier responses that resemble random guesses (Bays, Wu, & Husain, 2011; Ma et al., 2014; Nilakantan et al., 2018; Richter et al., 2016; Zhang & Luck, 2008, 2009), allowing for novel investigations of an underexplored feature type in this domain.

Though we are hopeful that VCS space will be useful to many researchers, we are not suggesting that stimulus selection should only ever be limited to validated circular spaces. Naturalistic stimuli such as videos or real-world images may be more generalizable than the simple colors, dots, lines, and words commonly used in many experiments. However, naturalistic stimuli also have their drawbacks, including the lack of precise experimenter control for factors such as visual similarity. Though time consuming, the development of complex stimulus spaces well-validated on different types of subjective similarity may be one method to include both the needed complexity of naturalistic stimuli and the needed experimenter control of extraneous factors. Indeed, emerging research has begun characterizing highly complex multidimensional spaces for faces (Busey, 1998; Chang, Nemrodov, Lee, & Nestor, 2017; Hopper, Finklea, Winkielman, & Huber, 2014; Nestor, Plaut, & Behrmann, 2016), real-world objects (Frank, Gray, &

Montaldi, 2019; Hebart et al., 2019; Hout, Goldinger, & Brady, 2014; Migo, Montaldi, & Mayes, 2013), and methods to expedite the validation of stimulus spaces (Hout, Cunningham, Robbins, & MacDonald, 2018; Kriegeskorte & Mur, 2012). Complementing this emerging direction of research, VCS space is the first tool comparable to circular color space, allowing researchers explicit control over the visual similarity of shape.

References

Abbott, J. T., Griffiths, T. L., & Regier, T. (2016). Focal colors across languages are representative members of color categories. *Proceedings of the National Academy of Sciences of the United States of America, 113,* 11178–11183. http://dx.doi.org/10.1073/pnas.1513298113

Abla, D., & Okanoya, K. (2009). Visual statistical learning of shape sequences: An ERP study. *Neuroscience Research, 64,* 185–190. http://dx.doi.org/10.1016/j.neures.2009.02.013

Aldrich, K. M., Hellier, E. J., & Edworthy, J. (2009). What determines auditory similarity? The effect of stimulus group and methodology. *Quarterly Journal of Experimental Psychology, 62,* 63–83. http://dx.doi.org/10.1080/17470210701814451

Apthorp, D., & Bell, J. (2015). Symmetry is less than meets the eye. *Current Biology, 25*(7), R267–R268. http://dx.doi.org/10.1016/j.cub.2015.02.017

Attneave, F. (1950). Dimensions of similarity. *The American Journal of Psychology, 63,* 516–556. http://dx.doi.org/10.2307/1418869

Bar, M., & Neta, M. (2006). Humans prefer curved visual objects. *Psychological Science, 17,* 645–648. http://dx.doi.org/10.1111/j.1467-9280.2006.01759.x

Bays, P. M., Wu, E. Y., & Husain, M. (2011). Storage and binding of object features in visual working memory. *Neuropsychologia, 49,* 1622–1631. http://dx.doi.org/10.1016/j.neuropsychologia.2010.12.023

Becker, S. I., Folk, C. L., & Remington, R. W. (2013). Attentional capture does not depend on feature similarity, but on target-nontarget relations. *Psychological Science, 24,* 634–647. http://dx.doi.org/10.1177/0956797612458528

Bell, J., Hancock, S., Kingdom, F. A. A., & Peirce, J. W. (2010). Global shape processing: Which parts form the whole? *Journal of Vision, 10*(6), 16. http://dx.doi.org/10.1167/10.6.16

Brincat, S. L., & Connor, C. E. (2004). Underlying principles of visual shape selectivity in posterior inferotemporal cortex. *Nature Neuroscience, 7,* 880–886. http://dx.doi.org/10.1038/nn1278

Brouwer, G. J., & Heeger, D. J. (2009). Decoding and reconstructing color from responses in human visual cortex. *The Journal of Neuroscience, 29,* 13992–14003. http://dx.doi.org/10.1523/JNEUROSCI.3577-09.2009

Brouwer, G. J., & Heeger, D. J. (2013). Categorical clustering of the neural representation of color. *The Journal of Neuroscience, 33,* 15454–15465. http://dx.doi.org/10.1523/JNEUROSCI.2472-13.2013

Brown, W. R. J., & MacAdam, D. L. (1949). Visual sensitivities to combined chromaticity and luminance differences. *Journal of the Optical Society of America, 39,* 808–834. http://dx.doi.org/10.1364/JOSA.39.000808

Busey, T. A. (1998). Physical and psychological representations of faces: Evidence from morphing. *Psychological Science, 9,* 476–483. http://dx.doi.org/10.1111/1467-9280.00088

Cacciamani, L., Scalf, P. E., & Peterson, M. A. (2015). Neural evidence for competition-mediated suppression in the perception of a single object. *Cortex: A Journal Devoted to the Study of the Nervous System and Behavior, 72,* 124–139. http://dx.doi.org/10.1016/j.cortex.2015.05.018

Chang, C.-H., Nemrodov, D., Lee, A. C. H., & Nestor, A. (2017). Memory and perception-based facial image reconstruction. *Scientific Reports, 7,* 6499. http://dx.doi.org/10.1038/s41598-017-06585-2

Charest, I., Kievit, R. A., Schmitz, T. W., Deca, D., & Kriegeskorte, N. (2014). Unique semantic space in the brain of each beholder predicts perceived similarity. *Proceedings of the National Academy of Sciences of the United States of America, 111,* 14565–14570. http://dx.doi.org/10.1073/pnas.1402594111

Chen, Y.-C., Huang, P.-C., Woods, A., & Spence, C. (2016). When "Bouba" equals "Kiki": Cultural commonalities and cultural differences in sound-shape correspondences. *Scientific Reports, 6,* 26681. http://dx.doi.org/10.1038/srep26681

Cheung, V. (2016). Uniform color spaces. In J. Chen, W. Cranton, & M. Fihn (Eds.), *Handbook of visual display technology* (pp. 187–196). Heidelberg, Germany: Springer. http://dx.doi.org/10.1007/978-3-319-14346-0_14

Connor, C. E., Egeth, H. E., & Yantis, S. (2004). Visual attention: Bottom-up versus top-down. *Current Biology, 14*(19), R850–R852. http://dx.doi.org/10.1016/j.cub.2004.09.041

Cooper, R. A., & Ritchey, M. (2019). Cortico-hippocampal network connections support the multidimensional quality of episodic memory. *eLife, 8,* e45591. http://dx.doi.org/10.7554/eLife.45591

Corey, D. M., Dunlap, W. P., & Burke, M. J. (1998). Averaging correlations: Expected values and bias in combined Pearson rs and Fisher's z transformations. *Journal of General Psychology, 125,* 245–261. http://dx.doi.org/10.1080/00221309809595548

Davis, T., Xue, G., Love, B. C., Preston, A. R., & Poldrack, R. A. (2014). Global neural pattern similarity as a common basis for categorization and recognition memory. *The Journal of Neuroscience, 34,* 7472–7484. http://dx.doi.org/10.1523/JNEUROSCI.3376-13.2014

Drucker, D. M., & Aguirre, G. K. (2009). Different spatial scales of shape similarity representation in lateral and ventral LOC. *Cerebral Cortex, 19,* 2269–2280. http://dx.doi.org/10.1093/cercor/bhn244

Drucker, D. M., Kerr, W. T., & Aguirre, G. K. (2009). Distinguishing conjoint and independent neural tuning for stimulus features with fMRI adaptation. *Journal of Neurophysiology, 101,* 3310–3324. http://dx.doi.org/10.1152/jn.91306.2008

Duncan, J., & Humphreys, G. W. (1989). Visual search and stimulus similarity. *Psychological Review, 96,* 433–458. http://dx.doi.org/10.1037/0033-295X.96.3.433

El-Shamayleh, Y., & Pasupathy, A. (2016). Contour curvature as an invariant code for objects in visual area V4. *The Journal of Neuroscience, 36,* 5532–5543. http://dx.doi.org/10.1523/JNEUROSCI.4139-15.2016

Ezzyat, Y., & Davachi, L. (2014). Similarity breeds proximity: Pattern similarity within and across contexts is related to later mnemonic judgments of temporal proximity. *Neuron, 81,* 1179–1189. http://dx.doi.org/10.1016/j.neuron.2014.01.042

Feldman, J. (2000). Bias toward regular form in mental shape spaces. *Journal of Experimental Psychology: Human Perception and Performance, 26,* 152–165. http://dx.doi.org/10.1037/0096-1523.26.1.152

Firestone, C., & Scholl, B. J. (2014). "Please tap the shape, anywhere you like": Shape skeletons in human vision revealed by an exceedingly simple measure. *Psychological Science, 25,* 377–386. http://dx.doi.org/10.1177/0956797613507584

Frank, D., Gray, O., & Montaldi, D. (2019). SOLID-Similar object and lure image database. *Behavior Research Methods*. Advance online publication. http://dx.doi.org/10.3758/s13428-019-01211-7

Fukuda, K., Awh, E., & Vogel, E. K. (2010). Discrete capacity limits in visual working memory. *Current Opinion in Neurobiology, 20,* 177–182. http://dx.doi.org/10.1016/j.conb.2010.03.005

Fusco, N. (2015). The quantitative isoperimetric inequality and related topics. *Bulletin of Mathematical Sciences, 5,* 517–607. http://dx.doi.org/10.1007/s13373-015-0074-x

Gallant, J. L., Braun, J., & Van Essen, D. C. (1993). Selectivity for polar, hyperbolic, and Cartesian gratings in macaque visual cortex. *Science, 259,* 100–103. http://dx.doi.org/10.1126/science.8418487

Gallant, J. L., Connor, C. E., Rakshit, S., Lewis, J. W., & Van Essen, D. C. (1996). Neural responses to polar, hyperbolic, and Cartesian gratings in

area V4 of the macaque monkey. *Journal of Neurophysiology, 76,* 2718–2739. http://dx.doi.org/10.1152/jn.1996.76.4.2718

Gardner, J. L., & Liu, T. (2019). Inverted encoding models reconstruct an arbitrary model response, not the stimulus. *eNeuro*. Advance online publication. http://dx.doi.org/10.1523/ENEURO.0363-18.2019

Garner, W. R., & Felfoldy, G. L. (1970). Integrality of stimulus dimensions in various types of information processing. *Cognitive Psychology, 1,* 225–241. http://dx.doi.org/10.1016/0010-0285(70)90016-2

Goldstone, R. L. (1994). The role of similarity in categorization: Providing a groundwork. *Cognition, 52,* 125–157. http://dx.doi.org/10.1016/0010-0277(94)90065-5

Grau, J. W., & Kemler Nelson, D. G. (1988). The distinction between integral and separable dimensions: Evidence for the integrality of pitch and loudness. *Journal of Experimental Psychology: General, 117,* 347–370. http://dx.doi.org/10.1037/0096-3445.117.4.347

Grill-Spector, K., Kourtzi, Z., & Kanwisher, N. (2001). The lateral occipital complex and its role in object recognition. *Vision Research, 41,* 1409–1422. http://dx.doi.org/10.1016/S0042-6989(01)00073-6

Guerrieri, F., Schubert, M., Sandoz, J.-C., & Giurfa, M. (2005). Perceptual and neural olfactory similarity in honeybees. *PLoS Biology, 3*(4), e60. http://dx.doi.org/10.1371/journal.pbio.0030060

Guild, J. (1931). The colorimetric properties of the spectrum. *Philosophical Transactions of the Royal Society of London, 230*(A), 149–187. http://dx.doi.org/10.1098/rsta.1932.0005

Hanczakowski, M., Beaman, C. P., & Jones, D. M. (2017). When distraction benefits memory through semantic similarity. *Journal of Memory and Language, 94,* 61–74. http://dx.doi.org/10.1016/j.jml.2016.11.005

Hanson-Vaux, G., Crisinel, A. S., & Spence, C. (2013). Smelling shapes: Crossmodal correspondences between odors and shapes. *Chemical Senses, 38,* 161–166. http://dx.doi.org/10.1093/chemse/bjs087

Haushofer, J., Livingstone, M. S., & Kanwisher, N. (2008). Multivariate patterns in object-selective cortex dissociate perceptual and physical shape similarity. *PLoS Biology, 6*(7), e187. http://dx.doi.org/10.1371/journal.pbio.0060187

Hebart, M. N., Dickter, A. H., Kidder, A., Kwok, W. Y., Corriveau, A., van Wicklin, C., & Baker, C. I. (2019). THINGS: A database of 1,854 object concepts and more than 26,000 naturalistic object images. *bioRxiv*. Advance online publication. http://dx.doi.org/10.1101/545954

Hopper, W. J., Finklea, K. M., Winkielman, P., & Huber, D. E. (2014). Measuring sexual dimorphism with a race-gender face space. *Journal of Experimental Psychology: Human Perception and Performance, 40,* 1779–1788. http://dx.doi.org/10.1037/a0037743

Hout, M. C., Cunningham, C. A., Robbins, A., & MacDonald, J. (2018). Simulating the fidelity of data for large stimulus set sizes and variable dimension estimation in multidimensional scaling. *SAGE Open*. Advance online publication. http://dx.doi.org/10.1177/2158244018773143

Hout, M. C., Godwin, H. J., Fitzsimmons, G., Robbins, A., Menneer, T., & Goldinger, S. D. (2016). Using multidimensional scaling to quantify similarity in visual search and beyond. *Attention, Perception & Psychophysics, 78,* 3–20. http://dx.doi.org/10.3758/s13414-015-1010-6

Hout, M. C., Goldinger, S. D., & Brady, K. J. (2014). MM-MDS: A multidimensional scaling database with similarity ratings for 240 object categories from the Massive Memory picture database. *PLoS ONE, 9*(11), e112644. http://dx.doi.org/10.1371/journal.pone.0112644

Hout, M. C., Goldinger, S. D., & Ferguson, R. W. (2013). The versatility of SpAM: A fast, efficient, spatial method of data collection for multidimensional scaling. *Journal of Experimental Psychology: General, 142,* 256–281. http://dx.doi.org/10.1037/a0028860

Hout, M. C., Papesh, M. H., & Goldinger, S. D. (2013). Multidimensional scaling. *WIREs Cognitive Science, 4,* 93–103. http://dx.doi.org/10.1002/wcs.1203

Hung, C.-C., Carlson, E. T., & Connor, C. E. (2012). Medial axis shape coding in macaque inferotemporal cortex. *Neuron, 74,* 1099–1113. http://dx.doi.org/10.1016/j.neuron.2012.04.029

Jiang, X., Bradley, E., Rini, R. A., Zeffiro, T., Vanmeter, J., & Riesenhuber, M. (2007). Categorization training results in shape- and category-selective human neural plasticity. *Neuron, 53,* 891–903. http://dx.doi.org/10.1016/j.neuron.2007.02.015

Jiang, Y. V., Lee, H. J., Asaad, A., & Remington, R. (2016). Similarity effects in visual working memory. *Psychonomic Bulletin & Review, 23,* 476–482. http://dx.doi.org/10.3758/s13423-015-0905-5

Jozwik, K. M., Kriegeskorte, N., & Mur, M. (2016). Visual features as stepping stones toward semantics: Explaining object similarity in IT and perception with non-negative least squares. *Neuropsychologia, 83,* 201–226. http://dx.doi.org/10.1016/j.neuropsychologia.2015.10.023

Kaneshiro, B., Perreau Guimaraes, M., Kim, H.-S., Norcia, A. M., & Suppes, P. (2015). A representational similarity analysis of the dynamics of object processing using single-trial EEG classification. *PLoS ONE, 10*(8), e0135697. http://dx.doi.org/10.1371/journal.pone.0135697

Kemler Nelson, D. G. (1993). Processing integral dimensions: The whole view. *Journal of Experimental Psychology: Human Perception and Performance, 19,* 1105–1113. http://dx.doi.org/10.1037/0096-1523.19.5.1105

Kesavan, S. (2002). The isoperimetric inequality. *Resonance, 7,* 8–18. http://dx.doi.org/10.1007/BF02836181

Kleiner, M., Brainard, D., & Pelli, D. (2007). What's new in Psychtoolbox-3? *Perception, 36,* 1–16.

Kok, P., & Turk-Browne, N. B. (2018). Associative prediction of visual shape in the hippocampus. *The Journal of Neuroscience, 38,* 6888–6899. http://dx.doi.org/10.1523/JNEUROSCI.0163-18.2018

Kourtzi, Z., & Kanwisher, N. (2000). Cortical regions involved in perceiving object shape. *The Journal of Neuroscience, 20,* 3310–3318. http://dx.doi.org/10.1523/JNEUROSCI.20-09-03310.2000

Kriegeskorte, N., & Kievit, R. A. (2013). Representational geometry: Integrating cognition, computation, and the brain. *Trends in Cognitive Sciences, 17,* 401–412. http://dx.doi.org/10.1016/j.tics.2013.06.007

Kriegeskorte, N., & Mur, M. (2012). Inverse MDS: Inferring dissimilarity structure from multiple item arrangements. *Frontiers in Psychology, 3,* 245. http://dx.doi.org/10.3389/fpsyg.2012.00245

Kriegeskorte, N., Mur, M., & Bandettini, P. (2008). Representational similarity analysis - connecting the branches of systems neuroscience. *Frontiers in Systems Neuroscience, 2,* 4. http://dx.doi.org/10.3389/neuro.06.004.2008

Labrecque, L. I., & Milne, G. R. (2012). Exciting red and competent blue: The importance of color in marketing. *Journal of the Academy of Marketing Science, 40,* 711–727. http://dx.doi.org/10.1007/s11747-010-0245-y

Larkey, L. B., & Markman, A. B. (2005). Processes of similarity judgment. *Cognitive Science, 29,* 1061–1076. http://dx.doi.org/10.1207/s15516709cog0000_30

Li, A. Y., Fidalgo, C. O., Liang, J., Lee, A. C. H., & Barense, M. D. (2018). *Examining the impact of item-distractor similarity using a validated circular shape space*. Poster session presented at the Annual Meeting of the Vision Sciences Society, St. Petersburg Beach, Florida.

Li, A. Y., Liang, J., Lee, A. C. H., & Barense, M. D. (2019). Visual interference can help and hinder memory: Measuring memory fidelity using a novel circular shape space. *bioRxiv*. Advance online publication. http://dx.doi.org/10.1101/535922

Lin, P.-H., & Luck, S. J. (2009). The influence of similarity on visual working memory representations. *Visual Cognition, 17,* 356–372. http://dx.doi.org/10.1080/13506280701766313

Loffler, G. (2008). Perception of contours and shapes: Low and intermediate stage mechanisms. *Vision Research, 48,* 2106–2127. http://dx.doi.org/10.1016/j.visres.2008.03.006

Ma, W. J., Husain, M., & Bays, P. M. (2014). Changing concepts of working memory. *Nature Neuroscience, 17,* 347–356. http://dx.doi.org/10.1038/nn.3655

Martin, C. B., Douglas, D., Newsome, R. N., Man, L. L. Y., & Barense, M. D. (2018). Integrative and distinctive coding of visual and conceptual object features in the ventral visual stream. *eLife, 7,* e31873. http://dx.doi.org/10.7554/eLife.31873

McDermott, K. C., & Webster, M. A. (2012). Uniform color spaces and natural image statistics. *Journal of the Optical Society of America A, Optics, Image Science, and Vision, 29*(2), A182–A187. http://dx.doi.org/10.1364/JOSAA.29.00A182

Migo, E. M., Montaldi, D., & Mayes, A. R. (2013). A visual object stimulus database with standardized similarity information. *Behavior Research Methods, 45,* 344–354. http://dx.doi.org/10.3758/s13428-012-0255-4

Mur, M., Meys, M., Bodurka, J., Goebel, R., Bandettini, P. A., & Kriegeskorte, N. (2013). Human object-similarity judgments reflect and transcend the primate-IT object representation. *Frontiers in Psychology, 4,* 128. http://dx.doi.org/10.3389/fpsyg.2013.00128

Nandy, A. S., Sharpee, T. O., Reynolds, J. H., & Mitchell, J. F. (2013). The fine structure of shape tuning in area V4. *Neuron, 78,* 1102–1115. http://dx.doi.org/10.1016/j.neuron.2013.04.016

Nestor, A., Plaut, D. C., & Behrmann, M. (2016). Feature-based face representations and image reconstruction from behavioral and neural data. *Proceedings of the National Academy of Sciences of the United States of America, 113,* 416–421. http://dx.doi.org/10.1073/pnas.1514551112

Nilakantan, A. S., Bridge, D. J., VanHaerents, S., & Voss, J. L. (2018). Distinguishing the precision of spatial recollection from its success: Evidence from healthy aging and unilateral mesial temporal lobe resection. *Neuropsychologia, 119,* 101–106. http://dx.doi.org/10.1016/j.neuropsychologia.2018.07.035

Novick, L. R. (1988). Analogical transfer, problem similarity, and expertise. *Journal of Experimental Psychology: Learning, Memory, and Cognition, 14,* 510–520. http://dx.doi.org/10.1037/0278-7393.14.3.510

Offenbach, S. I. (1990). Integral and separable dimensions of shape. *Bulletin of the Psychonomic Society, 28,* 30–32. http://dx.doi.org/10.3758/BF03337640

Op de Beeck, H. P., Torfs, K., & Wagemans, J. (2008). Perceived shape similarity among unfamiliar objects and the organization of the human object vision pathway. *The Journal of Neuroscience, 28,* 10111–10123. http://dx.doi.org/10.1523/JNEUROSCI.2511-08.2008

Op de Beeck, H., Wagemans, J., & Vogels, R. (2001). Inferotemporal neurons represent low-dimensional configurations of parameterized shapes. *Nature Neuroscience, 4,* 1244–1252. http://dx.doi.org/10.1038/nn767

Osserman, R. (1978). The isoperimetric inequality. *Bulletin of the American Mathematical Society, 84,* 1182–1239. http://dx.doi.org/10.1090/S0002-9904-1978-14553-4

Pasupathy, A. (2006). Neural basis of shape representation in the primate brain. *Progress in Brain Research, 154,* 293–313. http://dx.doi.org/10.1016/S0079-6123(06)54016-6

Pasupathy, A., & Connor, C. E. (2002). Population coding of shape in area V4. *Nature Neuroscience, 5,* 1332–1338. http://dx.doi.org/10.1038/972

Pasupathy, A., El-Shamayleh, Y., & Popovkina, D. V. (2018). Visual shape and object perception. *Neuroscience*. Advance online publication. http://dx.doi.org/10.1093/acrefore/9780190264086.013.75

Peirce, J. W. (2015). Understanding mid-level representations in visual processing. *Journal of Vision, 15*(7), 5. http://dx.doi.org/10.1167/15.7.5

Peterson, M. A., & Gibson, B. S. (1994). Object recognition contributions to figure-ground organization: Operations on outlines and subjective contours. *Perception & Psychophysics, 56,* 551–564. http://dx.doi.org/10.3758/BF03206951

Pfaffmann, C., Bartoshuk, L. M., & McBurney, D. H. (1971). Taste psychophysics. In L. M. Beidler (Ed.), *Taste: Handbook of sensory physiology* (pp. 75–101). Berlin, Germany: Springer. http://dx.doi.org/10.1007/978-3-642-65245-5_5

Pointer, M. R. (1981). A comparison of the CIE 1976 colour spaces. *Color Research and Application, 6,* 108–118. http://dx.doi.org/10.1002/col.5080060212

Ponce, C. R., Hartmann, T. S., & Livingstone, M. S. (2017). End-stopping predicts curvature tuning along the ventral stream. *The Journal of Neuroscience, 37,* 648–659. http://dx.doi.org/10.1523/JNEUROSCI.2507-16.2016

Pothos, E. M., Busemeyer, J. R., & Trueblood, J. S. (2013). A quantum geometric model of similarity. *Psychological Review, 120,* 679–696. http://dx.doi.org/10.1037/a0033142

Reber, R., Schwarz, N., & Winkielman, P. (2004). Processing fluency and aesthetic pleasure: Is beauty in the perceiver's processing experience? *Personality and Social Psychology Review, 8,* 364–382. http://dx.doi.org/10.1207/s15327957pspr0804_3

Regier, T., Kay, P., & Khetarpal, N. (2007). Color naming reflects optimal partitions of color space. *Proceedings of the National Academy of Sciences of the United States of America, 104,* 1436–1441. http://dx.doi.org/10.1073/pnas.0610341104

Richter, F. R., Cooper, R. A., Bays, P. M., & Simons, J. S. (2016). Distinct neural mechanisms underlie the success, precision, and vividness of episodic memory. *eLife, 5,* e18260. http://dx.doi.org/10.7554/eLife.18260

Roberson, D., Davies, I., & Davidoff, J. (2000). Color categories are not universal: Replications and new evidence from a stone-age culture. *Journal of Experimental Psychology: General, 129,* 369–398. http://dx.doi.org/10.1037/0096-3445.129.3.369

Robertson, A. R. (1977). The CIE 1976 color-difference formulae. *Color Research and Application, 2,* 7–11. http://dx.doi.org/10.1002/j.1520-6378.1977.tb00104.x

Robertson, A. R. (1990). Historical development of CIE recommended color difference equations. *Color Research and Application, 15,* 167–170. http://dx.doi.org/10.1002/col.5080150308

Safdar, M., Cui, G., Kim, Y. J., & Luo, M. R. (2017). Perceptually uniform color space for image signals including high dynamic range and wide gamut. *Optics Express, 25,* 15131–15151. http://dx.doi.org/10.1364/OE.25.015131

Salmela, V. R., Henriksson, L., & Vanni, S. (2016). Radial frequency analysis of contour shapes in the visual cortex. *PLoS Computational Biology, 12*(2), e1004719. http://dx.doi.org/10.1371/journal.pcbi.1004719

Salmela, V. R., Mäkelä, T., & Saarinen, J. (2010). Human working memory for shapes of radial frequency patterns. *Vision Research, 50,* 623–629. http://dx.doi.org/10.1016/j.visres.2010.01.014

Sanguinetti, J. L., Allen, J. J. B., & Peterson, M. A. (2014). The ground side of an object: Perceived as shapeless yet processed for semantics. *Psychological Science, 25,* 256–264. http://dx.doi.org/10.1177/0956797613502814

Schmidtmann, G., & Fruend, I. (2019). Radial frequency patterns describe a small and perceptually distinct subset of all possible planar shapes. *Vision Research, 154,* 122–130. http://dx.doi.org/10.1016/j.visres.2018.10.007

Schurgin, M. W., Wixted, J. T., & Brady, T. F. (2018). Psychophysical scaling reveals a unified theory of visual memory strength. *bioRxiv*. Advance online publication. http://dx.doi.org/10.1101/325472

Seo, H. S., Arshamian, A., Schemmer, K., Scheer, I., Sander, T., Ritter, G., & Hummel, T. (2010). Cross-modal integration between odors and abstract symbols. *Neuroscience Letters, 478,* 175–178. http://dx.doi.org/10.1016/j.neulet.2010.05.011

Shepard, R. N. (1980). Multidimensional scaling, tree-fitting, and clustering. *Science, 210,* 390–398. http://dx.doi.org/10.1126/science.210.4468.390

Skedung, L., Arvidsson, M., Chung, J. Y., Stafford, C. M., Berglund, B., & Rutland, M. W. (2013). Feeling small: Exploring the tactile perception limits. *Scientific Reports, 3,* 2617. http://dx.doi.org/10.1038/srep02617

Spence, C., & Ngo, M. K. (2012). Assessing the shape symbolism of the taste, flavour, and texture of foods and beverages. *Flavour, 1,* 12. http://dx.doi.org/10.1186/2044-7248-1-12

Sprague, T. C., Adam, K. C. S., Foster, J. J., Rahmati, M., Sutterer, D. W., & Vo, V. A. (2018). Inverted encoding models assay population-level stimulus representations, not single-unit neural tuning. *eNeuro*. Advance online publication. http://dx.doi.org/10.1523/ENEURO.0098-18.2018

Sun, S. Z., Fidalgo, C., Barense, M. D., Lee, A. C. H., Cant, J. S., & Ferber, S. (2017). Erasing and blurring memories: The differential impact of interference on separate aspects of forgetting. *Journal of Experimental Psychology: General, 146,* 1606–1630. http://dx.doi.org/10.1037/xge0000359

Taylor, C., Clifford, A., & Franklin, A. (2013). Color preferences are not universal. *Journal of Experimental Psychology: General, 142,* 1015–1027. http://dx.doi.org/10.1037/a0030273

Turoman, N., Velasco, C., Chen, Y.-C., Huang, P.-C., & Spence, C. (2018). Symmetry and its role in the crossmodal correspondence between shape and taste. *Attention, Perception, & Psychophysics, 80,* 738–751. http://dx.doi.org/10.3758/s13414-017-1463-x

Tversky, A. (1977). Features of similarity. *Psychological Review, 84,* 327–352. http://dx.doi.org/10.1037/0033-295X.84.4.327

Velasco, C., Woods, A. T., Petit, O., Cheok, A. D., & Spence, C. (2016). Crossmodal correspondences between taste and shape, and their implications for product packaging: A review. *Food Quality and Preference, 52,* 17–26. http://dx.doi.org/10.1016/j.foodqual.2016.03.005

Verheyen, S., Voorspoels, W., Vanpaemel, W., & Storms, G. (2016). Caveats for the spatial arrangement method: Comment on Hout, Goldinger, and Ferguson (2013). *Journal of Experimental Psychology: General, 145,* 376–382. http://dx.doi.org/10.1037/a0039758

Wardle, S. G., Kriegeskorte, N., Grootswagers, T., Khaligh-Razavi, S. M., & Carlson, T. A. (2016). Perceptual similarity of visual patterns predicts dynamic neural activation patterns measured with MEG. *NeuroImage, 132,* 59–70. http://dx.doi.org/10.1016/j.neuroimage.2016.02.019

Whitney, D., & Yamanashi Leib, A. (2018). Ensemble perception. *Annual Review of Psychology, 69,* 105–129. http://dx.doi.org/10.1146/annurev-psych-010416-044232

Wilken, P., & Ma, W. J. (2004). A detection theory account of change detection. *Journal of Vision, 4*(11), 20–35. http://dx.doi.org/10.1167/4.12.11

Wilson, H. R., & Wilkinson, F. (2015). From orientations to objects: Configural processing in the ventral stream. *Journal of Vision, 15*(7), 4. http://dx.doi.org/10.1167/15.7.4

Wright, W. D. (1929). A re-determination of the trichromatic coefficients of the spectral colours. *Transactions from the Optical Society, 30,* 141–164. http://dx.doi.org/10.1088/1475-4878/30/4/301

Xiberpix. (2008). SqirlzMorph [Computer software]. Retrieved from http://www.xiberpix.net/

Yassa, M. A., & Stark, C. E. L. (2011). Pattern separation in the hippocampus. *Trends in Neurosciences, 34,* 515–525. http://dx.doi.org/10.1016/j.tins.2011.06.006

Yonelinas, A. P. (2013). The hippocampus supports high-resolution binding in the service of perception, working memory and long-term memory. *Behavioural Brain Research, 254,* 34–44. http://dx.doi.org/10.1016/j.bbr.2013.05.030

Yue, X., Pourladian, I. S., Tootell, R. B. H., & Ungerleider, L. G. (2014). Curvature-processing network in macaque visual cortex. *Proceedings of the National Academy of Sciences of the United States of America, 111*(33), E3467–E3475. http://dx.doi.org/10.1073/pnas.1412616111

Zaslavsky, N., Kemp, C., Regier, T., & Tishby, N. (2018). Efficient compression in color naming and its evolution. *Proceedings of the National Academy of Sciences of the United States of America, 115,* 7937–7942. http://dx.doi.org/10.1073/pnas.1800521115

Zhang, W., & Luck, S. J. (2008). Discrete fixed-resolution representations in visual working memory. *Nature, 453,* 233–235. http://dx.doi.org/10.1038/nature06860

Zhang, W., & Luck, S. J. (2009). Sudden death and gradual decay in visual working memory. *Psychological Science, 20,* 423–428. http://dx.doi.org/10.1111/j.1467-9280.2009.02322.x

Received January 30, 2019
Revision received August 26, 2019
Accepted August 27, 2019 ■